The Thesis Committee for Daniel William Dykstra
Certifies that this is the approved version of the following thesis:

Elucidating Binding Modes of Zuonin A Enantiomers to JNK1 via *in silico* methods

APPROVED BY
SUPERVISING COMMITTEE:

Supervisor:

Pengyu Ren

Kevin Dalby

Elucidating Binding Modes of Zuonin A Enantiomers to JNK1 via *in silico* methods

by

Daniel William Dykstra, BS

Thesis

Presented to the Faculty of the Graduate School of

The University of Texas at Austin

in Partial Fulfillment

of the Requirements

for the Degree of

Master of Arts

The University of Texas at Austin

May 2013

Acknowledgements

I would like to thank Dr. Pengyu Ren for being both a mentor and a friend. I would also like to thank Dr. Kevin Dalby for his assistance and the rest of the Ren Lab.

Abstract

Elucidating Binding Modes of Zuonin A Enantiomers to JNK1 via *in silico* methods

Daniel William Dykstra, MA

The University of Texas at Austin, 2013

Supervisor: Pengyu Ren

Aberrant JNK signaling can result in two main forms of disease in humans: 1) neurological, coronary, hepatobiliary, and respiratory diseases and 2) autoimmune, inflammatory, and cancer conditions. Enantiomers of the lignan zuonin A, (-)-zuonin A and (+)-zuonin A, have been shown to bind to JNK isoforms with similar affinity and disrupt protein-protein interactions at JNK's D-recruitment site, making them a good candidate for specific non-ATP competitive inhibitors. However, (-)-zuonin A inhibits 80% of JNK catalyzed reactions at saturating levels, while (+)-zuonin A only inhibits 15%. Molecular docking and molecular dynamics simulations were performed to gain a better understanding of how these inhibitors interact JNK. The results of this study provide an alternative binding mode for (-)-zuonin A, compared to one proposed in a previous study, that shows (-)-zuonin A interacting with JNK via an induced fit mechanism by forming a larger pocket for itself near the highly conserved φA-X-φB recognition site, a dynamic move not seen in (+)-zuonin A simulations, and may help explain their different inhibition patterns.

Table of Contents

List of Tables

List of Figures

Chapter 1: Introduction

Mitogen Activated Protein (MAP) Kinases

Mitogen Activated Protein (MAP) kinases are a class of serine/threonine specific protein kinases that are highly conserved in eukaryotic organisms. These enzymes are most commonly members of a three tiered signal transduction cascade which uses a series of phosphorylation events to help relay "messages" from external stimuli to intracellular targets in order to elicit a desired cellular response.[1]

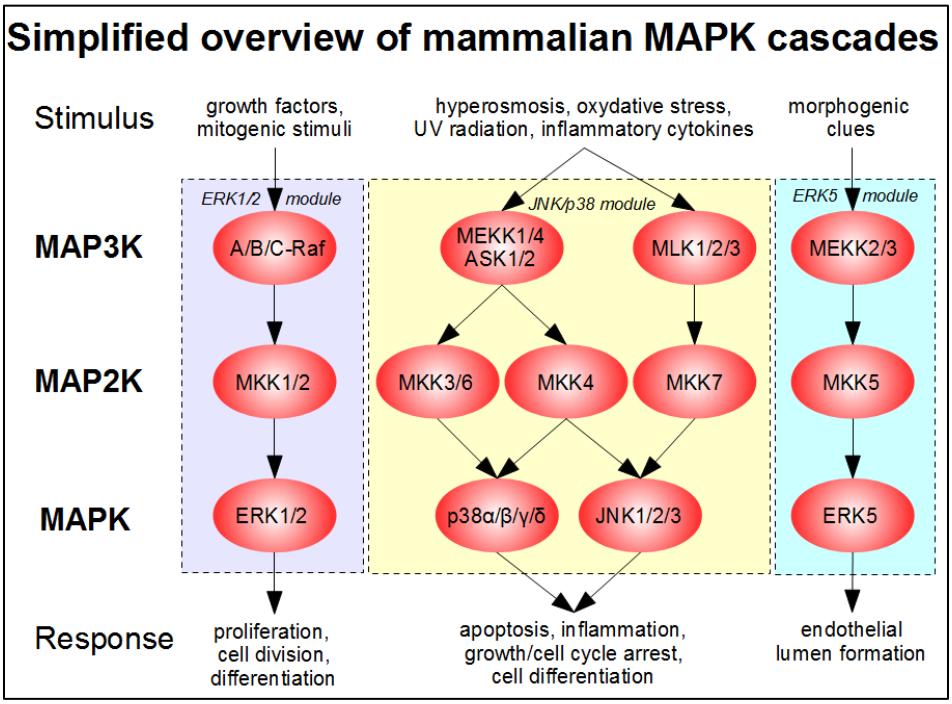

Figure 1: Overview of a mammalian MAP kinase cascade[2]

There are three main MAPK pathways in mammals, ERK1/2 (Extracellular-Signal-Regulated Kinases), ERK5, and p38/JNK (c-Jun N-terminal Kinases). ERK1/2 and ERK5 pathways are both activated by the binding of mitogens and growth factors at

cell surface receptors and regulate cellular proliferation, division, and differentiation. The p38/JNK pathway is activated in response to environmental stresses, such as hyperosmosis, oxidative stress, UV radiation and inflammatory cytokines, and can result in apoptosis, inflammation, cell cycle arrest, or cellular differentiation. Unfortunately, miscues in MAPK signaling can result in chronic diseases such as cancer, obesity, type-2 diabetes, inflammation and Alzheimer's disease.[3-6]

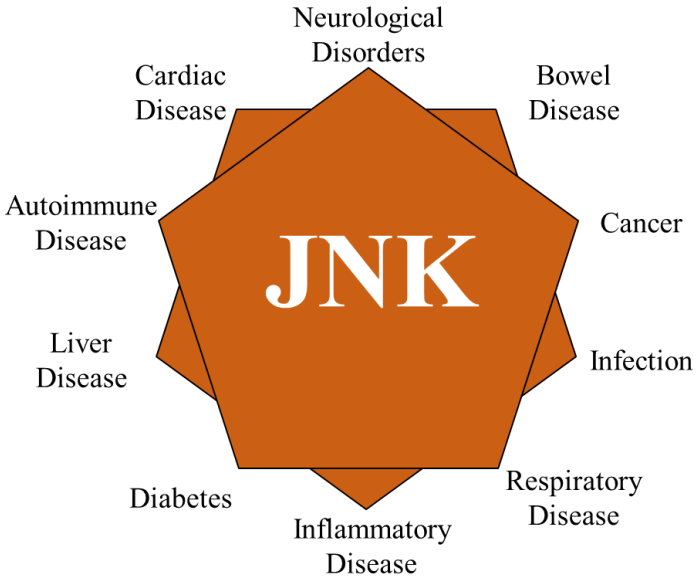

Figure 2: Diseases linked to aberrant JNK signalling

MAP kinases have the canonical core structure seen in other protein kinases. These features include two domains connected by a hinge region which allows for minor flexibility, an ATP binding pocket and substrate recognition site at the domain interface which help catalyze the transfer of ATP's gamma phosphate to the substrate's hydroxyl group, and an activation loop located in close proximity to the active site which determines the activation state of the kinase. The activation loop contains two phosphorylation sites in the form of a T-X-Y motif for MAP kinases.[1]

An interesting feature of MAP kinases is their use of docking regions to recruit, orient, and discriminate between activators, regulators, and substrates. The MAPK D-recruitment site (DRS) was of particular interest in this study. The DRS targets proteins and peptides containing a D-site motif via a negatively charged common docking (CD) domain and a hydrophobic groove. Successful binding to this region helps align the two proteins and increases the likelihood for the desired catalytic reaction.[7]

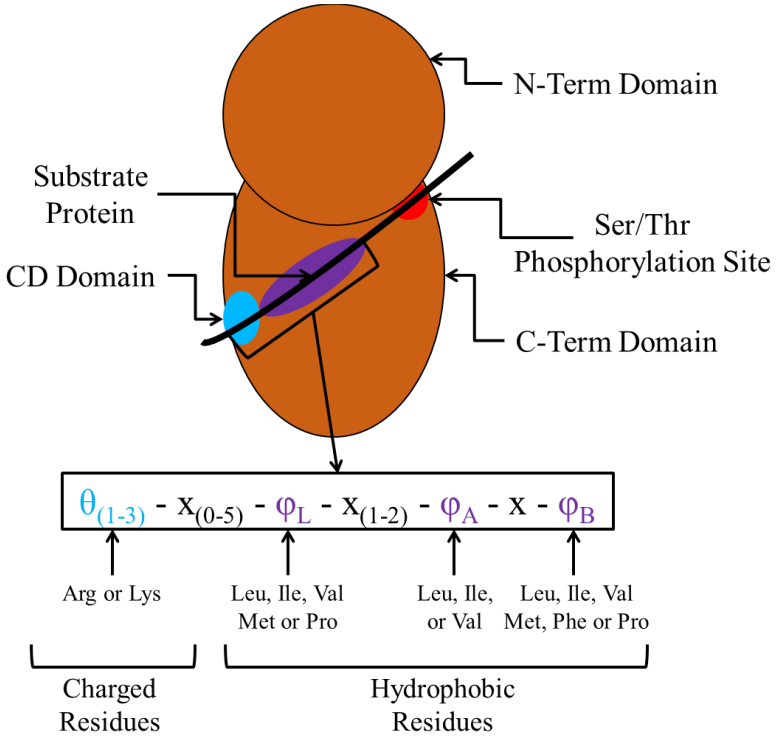

Figure 3: General MAPK structure with consensus D-site.

The positively charged amino acids, denoted as θ in figure 3, of the D-site interact with the negatively charged amino acids of the CD domain. In addition, the highly conserved hydrophobic residues, $\varphi_{L,A,B}$, form van der Waal's contacts with pockets formed along the hydrophobic groove.[7]

C-JUN N-TERMINAL KINASES (JNKS) AND THEIR ROLE IN DISEASE

JNKs are members of the MAP kinase family and play an integral role in eukaryotic cellular stress response mechanisms. JNK is encoded by genes *Jnk1*, *Jnk2*, and *Jnk3* and have 10 different splice variants. While JNK1 and JNK2 are ubiquitously expressed throughout the body, JNK3 is predominately localized to the brain, testis and heart. All isoforms are activated by dual phosphorylation of the Thr-Pro-Tyr motif located on the activation loop of the enzyme. The tyrosine and threonine residues are phosphorylated by upstream kinases MKK4 and MKK7 respectively.[3]

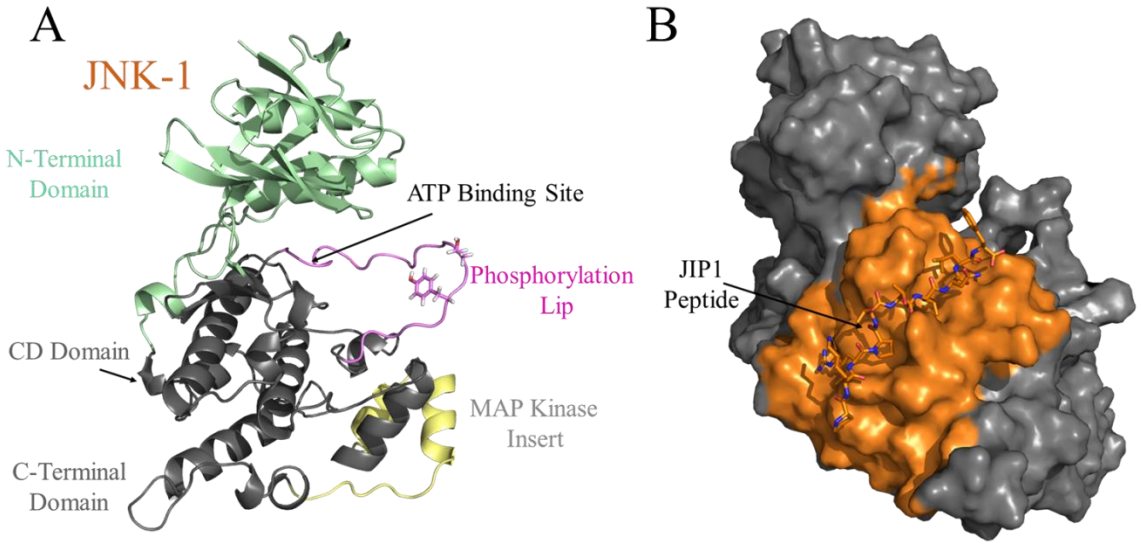

Figure 4: a) Anatomy of JNK1 b) JIP1 peptide bound to JNK1's D-recruitment site

Aberrant JNK signaling can result in two main forms of disease in humans: 1) neurological, coronary, hepatobiliary, and respiratory diseases and 2) autoimmune, inflammatory, and cancer conditions.

JNKs play a vital role proper in brain/neurological development. Single knockout studies of any JNK isoform, in addition to *Jnk1*/*Jnk3* and *Jnk2*/*Jnk3* double knockouts, had no deleterious effects on mouse development. However, the *Jnk1/Jnk2* double

knockout resulted in early embryonic termination due to unregulated apoptosis of neuronal cells in the brain. This suggests that JNK1 and JNK2 may have some redundant functions.

Contrary to their similar function in brain development, JNK1 and JNK2 appear to have separate roles in fibroblast proliferation and the progression of certain forms of cancer. Studies have shown that upregulation of JNK1 increases c-Jun phosphorylation and activation resulting in cellular proliferation, while the inverse is true for JNK2.

The diverse roles of JNKs in human pathogenesis make it a desirable drug target, however, finding the appropriate specificity amongst other kinases, let alone the JNK isoforms, has been a challenge.[4]

INHIBITION OF JNKS AND ZUONIN A

Two main strategies have been employed for the development of JNK inhibitors. ATP competitive inhibitors target the ATP binding pocket, as the name suggests, while non-ATP competitive inhibitors bind to the D-recruitment site and disrupt target substrate binding. One successful ATP competitive inhibitor, SP600125, has been proven to be effective at inhibiting JNK in both cell culture as well as mouse models. However, targeting the ATP binding site comes at the cost of reduced specificity due to the conserved nature and abundance of ATP binding pockets.[8] In addition, ATP competitive inhibitors must compete with high concentrations of intracellular ATP, which vary from 1-10 mM.

For these reasons, there has been a push to develop non-ATP competitive inhibitors. A JNK interacting protein-1 (JIP1) peptide fragment known to interact with the JNK D-recruitment site was able to selectively inhibit JNK over other similar MAP kinases such as ERK2 and p38, figure 4b. Unfortunately, the large number of degrees of

freedom of the peptide backbone and issues with bioavailability make peptide drugs a somewhat undesirable lead compound. To combat this issue, a library of small molecules was screened to reveal compounds capable of disrupting the JIP1 and JNK1 interaction. One potential lead discovered in this screen was BI-78D3. BI-78D3 confirmed that the concept of targeting the DRS using small molecules could potentially be effective by inhibiting the phosphorylation of JNK1 substrates in a dose dependent manner.[9]

In order to expand on the number of non-ATP competitive inhibitor scaffolds, a virtual screen was performed to compare BI-78D3 to other compounds based on three-dimensional shape and electrostatic similarities. One compound of interest isolated from this study was the lignan (-)-zuonin A, figure 5, which has a 100-fold greater selectivity toward inhibiting JNK–protein interactions over ERK2 and p38 MAPKα.[10]

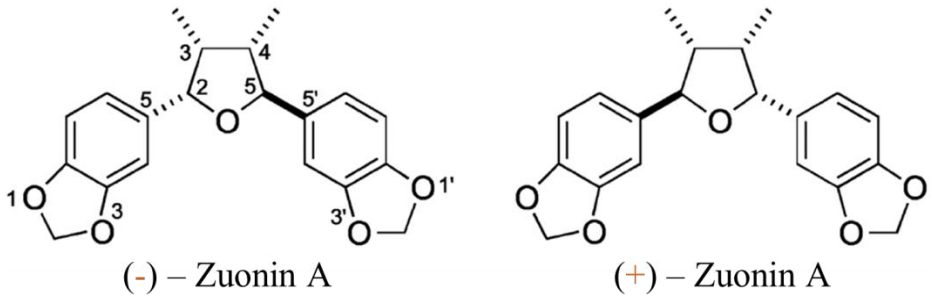

Figure 5: Chemical structure of zuonin A enantiomers

An interesting observation regarding (-)-zuonin A and its enantiomer, (+)-zuonin A, was that both were equally as effective at displacing pepJIP1 from JNK1 (IC_{50} of ~2.6 ± 0.2 μM), however, at saturating concentrations, (-)-zuonin A inhibited 80% the maximal phosphorylation reaction, whereas (+)-zuonin A only inhibited 15%. This information suggests that the two zuonin A enantiomers must interact with JNK1 in different manners and is the motivation for the subject matter of this thesis.[11]

COMPUTER AIDED DRUG DESIGN

Statistics from 2000 through 2007 show that it takes between 11.4 to 13.5 years for a company to take a small molecule drug to market at an approximate cost of $1.8 billion.[12] These economic challenges and vast improvements in computational technology have sparked innovation in the field of computer aided drug design (CADD) with the goal of increasing search efficiency while decreasing the necessary costs.

Virtual screening has experienced wide spread use in the field of medicinal chemistry due to their ability to quickly screen large libraries of compounds at very little cost. One such ligand-based screen is a ligand-ligand similarity search which compares a known bioactive ligand to a library of compounds and ranks them according to a defined property such as shape, electrostatic profile, and/or biological activity. A de novo search for ligands can also be performed using molecular docking. This process requires a model of the target structure which can be obtained by experiment (x-ray crystallography/NMR data) or generated using homology modeling software. In this method, ligands are allowed to move freely and change conformations in an attempt to best fit the inverse of a user defined pocket. The generated configurations are known as poses. Each pose is scored and ranked using a scoring function which is usually an over-simplified empirical force field. These scoring functions rely on empirical data sets of known binding affinities with solved structures to derive contribution weights for lipophilic effects, hydrogen bonds, and rotatable bonds.

Unfortunately, molecular docking has several inherent flaws. Since target proteins have little to no flexibility, it gives an unrealistic landscape for the ligand to dock into and becomes a larger issue as a protein becomes more dynamic. Most docking programs also give a “binding free energy” for each snapshot, when in actuality it is ensemble-averaged thermodynamic quantity including vibrational, rotational, and conformational

contributions. Also, since scoring function parameters are usually optimized to a certain set of known substrate-ligand interactions which can result in an unwanted bias toward interactions not included in the training set. Lastly, molecular docking scoring functions do a poor job accounting for entropy and solvent effects that can be critical for substrate ligand binding. Although the success rate of molecular docking can be increased by using multiple scoring functions and using consensus scores, there is much left to be desired.

Physics based molecular mechanics force fields in conjunction with molecular dynamics (MD) or Monte Carlo (MC) simulations have been implemented in the drug discovery process to ameliorate many of the issues seen in molecular docking experiments. These simulations allow for the inclusion of explicit water molecules, movement of all atoms in the system, including protein and solvent, and more rigorous interaction energies calculated from detailed molecular mechanics force fields. A molecular mechanics force field is the summation of all the bonded and non-bonded forces experienced by a particular atom and has the general form seen in following equation.

$$\mathrm{U} = \sum_{\text{bonds}} k_{\mathrm{r}} \left(\mathrm{r} + r_0\right)^2 + \sum_{\text{angles}} k_\theta \left(\theta + \theta_0\right)^2 + \sum_{\text{dihedrals}} k_\varphi \left[1 + \cos(n\varphi + \varphi_0)\right] + \sum_{\text{vdW atom i}} \sum_{\text{j}\neq\text{i}} 4\epsilon_{i,j} \left[\left(\frac{\sigma_{\mathrm{i,j}}}{r_{\mathrm{i,j}}}\right)^{12} - \left(\frac{\sigma_{\mathrm{i,j}}}{r_{\mathrm{i,j}}}\right)^{6}\right] + \sum_{\text{Elect atom i}} \sum_{\text{j}\neq\text{i}} \frac{q_{\mathrm{i}} q_{\mathrm{j}}}{\epsilon_0 r_{\mathrm{i,j}}}$$

Eq. 1: Generalized force field equation

The bonded terms include bond lengths and bond angles, which are both represented mathematically as springs, and dihedral angles, which are modeled as periodic waves. The non-bonded van der Waals forces are approximated using a

Lennard-Jones potential and long range electrostatic interactions are taken into account using Coulomb's Law.

Once the potential energy of an atom at given coordinates, r, has been determined, it's possible to calculate the forces, F, acting on each atom by taking the gradient of the potential energy at time, i.

$$\mathrm{F}(\mathrm{r}_i) = -\nabla \mathrm{U}(\mathrm{r}_i)$$

Eq. 2

Newton's second law of motion can be applied to determine the acceleration, A, of that atom at that given moment if the forces and mass of the atom are known.

$$\mathrm{A}(\mathrm{r}_i) = \mathrm{F}(\mathrm{r}_i)/\mathrm{m}$$

Eq. 3

Using a small time step, usually on the order of 1 to 2 femtoseconds for atomic models, one can determine the new position, of each atom after each step.

$$\mathrm{r}_{i+1} = \mathrm{r}_i + \mathrm{v}_i \Delta \mathrm{t} + {}^{1}/_{2}\, \mathrm{a} \Delta \mathrm{t}^2$$

Eq. 4

The potential energy is calculated once again and the process is then repeated until the user obtains a desired sample size. One benefit to using molecular dynamics simulations is that the resulting trajectory follows a Boltzmann distribution and can thus be used to calculate fundamental properties of the system by straight averaging.

Once a trajectory of a protein-ligand interaction is obtained, the Molecular Mechanics-Generalized Born (Poisson-Boltzmann) Surface Area, or MM-GB(PB)SA, implicit solvent method can be used to calculate the binding free energy of the ligand utilizing the thermodynamic cycle shown in figure.

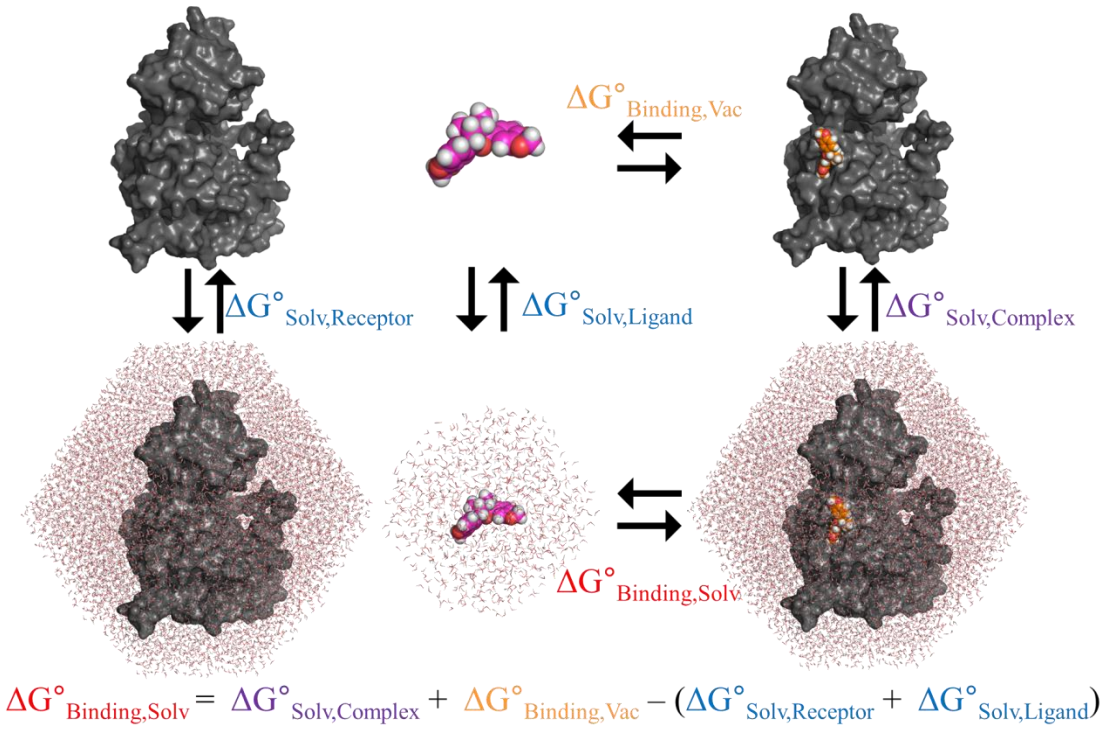

Figure 6: Thermodynamic cycle exploited to calculate solvated binding free energy ($\Delta G°_{Binding,Solv}$) using the MM-GBSA algorithm, where the grey JNK1 enzyme binds a zuonin A enantiomer to form a complex both in vacuum and solvent

Solvation free energies, ΔG_{Solv}, are the sum of the solvation energy of the polar contributions, $\Delta G_{Solv,polar}$, as determined using either the GB or PB method, and the solvation energy of the non-polar portion, $\Delta G_{Solv,nonpolar}$, was calculated using the surface area of the molecule.

$$\Delta G_{Solv} = \Delta G_{Solv,polar} + \Delta G_{Solv,non-polar}$$

Eq. 5

The binding free energy in a vacuum, $\Delta G_{Binding,Vac}$, is simply the sum of the change in enthalpy, $\Delta U_{MM,Vac}$, and entropy, $T\Delta S$, terms going from their respective unbound states to complex in the absence of solvent.

$$\Delta G_{Binding,Vac} = \Delta U_{MM,Vac} - T\Delta S$$

Eq. 6

Thus, the solvated binding free energy can be approximated by combining the previous equations to get:

$$\Delta G_{Binding,Solv} = \Delta U_{MM,Vac} + \Delta G_{GB} + \Delta G_{SA} - T\Delta S$$

Eq. 7

Where $\Delta U_{MM,Vac}$ is calculated using the molecular mechanics force field, ΔG_{GB} is the electrostatic (polar) solvation energy calculated using the Generalized-Born method, ΔG_{SA} is the nonpolar contributions to solvation energy based on the exposed surface area, and ΔS is the change in entropy which can be estimated using normal mode analysis and other methods.

The use of MD simulations ultimately gives the user a more accurate binding free energy by taking the ensemble average of a large number of potential conformations. In addition, each trajectory can be viewed using visualization software like VMD or PyMOL to give the user insight into what interactions and movements enhance binding the most.

Chapter 2: Experimental Design

IN SILICO REPRESENTATIONS OF JNK1 AND ZUONIN A

The dephosphorylated JNK1 structure used was previously generated by adding back missing amino acid residues to the crystal structure of the JNK1-JIP1 peptide complex (PDB ID: 1UKH)[8] using the homology software Modeler9v5[6]. Missing residues were far enough away from the proposed binding sites that they did not affect the initial docking experiments. Zuonin enantiomers were drawn using MarvinSketch and converted to 3D coordinates.

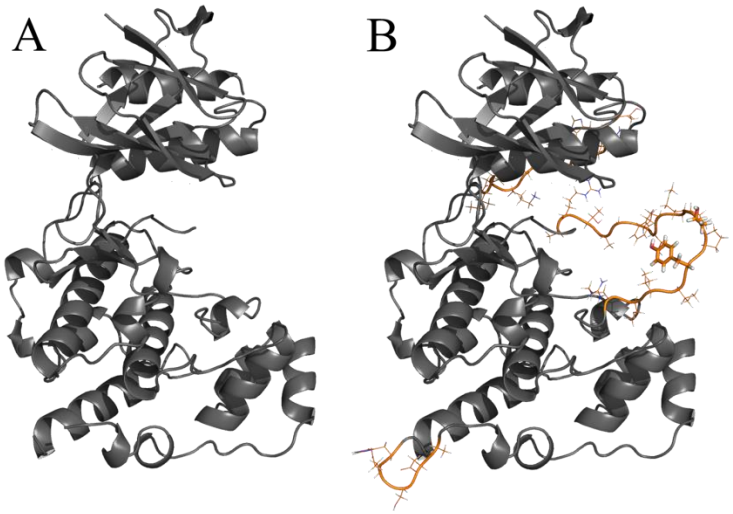

Figure 7: a) Crystal structure of JNK1 with missing residues (PDBID: 1UKH) b) Missing residues replaced in orange using Modeler9v5 with Thr183 & Tyr185 emphasized.

MOLECULAR DOCKING

Docking experiments were performed using Genetic Optimisation for Ligand Docking (GOLD) software provided by the Cambridge Crystallographic Data Centre (CCDC).[13] Both zuonin A enantiomers were docked 100 times into 10 different regions along the JNK-JIP1 interface yielding 1000 potential poses. The regions were defined as all JNK atoms within a 16Å radius of each JIP1 α-carbon to accommodate the

approximate width of zuonin (~14Å). Each docking began with an initial population of 200 members divided onto 5 islands. Crossover events were controlled using a niche size of 2 and a selection pressure of 1.1. The quality of fit for each pose was calculated using the Chemscore fitness function with the default parameters supplied by CCDC.

All docking poses were combined and clustered based on their RMSD calculated using GoldMine.[13] The highest scoring pose in each cluster was selected for the subsequent molecular dynamics simulation.

MOLECULAR DYNAMICS SIMULATIONS

Gaussian09 quantum mechanics software was used to optimize the 3D structure of zuonin and calculate accurate atomic charges.[14] The electrostatic potential for each atom was determined using the Merz-Singh-Kollman scheme.[15, 16] All calculations were performed using the Hartree-Fock/6-31G* basis set. The optimized structures were converted to Amber parameter and coordinate files using the antechamber and LEaP modules of Amber12 and the General Amber Force Field (GAFF).[17]

The topology and coordinate files for the zuonin-JNK1 complexes were created with LEaP using the ff99SB force field in conjunction with the previously generated parameter, coordinate and library files for zuonin. A set of topology and coordinate files were also created for the solvated system which consisted of a truncated octahedral TIP3P water box that extended 8Å from the enzyme's surface and added 4 Na+ counterions to balance the overall charge.

All minimization and MD equilibration steps were executed using the Sander module of Amber12 while production runs were performed using the PMEMD (Particle Mesh Ewald Molecular Dynamics) module. To remove any potential bad contacts, each system was minimized while holding the peptide backbone rigid until it converged to less

than 0.001 kcal/mole*Å. The steepest descent algorithm was used for the first 500 steps followed by 500 cycles of the conjugate gradient method.

The system was equilibrated using a two-step process. First, a 200ps NVT simulation was performed using a 2.0 fs integration timestep. The system was heated from 0K to 300K during the first 80ps and held constant for the remainder of the simulation. A second 1ns NPT equilibration step was executed at 1bar to equilibrate the size of the system. In both steps, all backbone atoms present in the original crystal structure were restrained while all other atoms were allowed to move freely.

An 8ns trajectory was acquired for each production run. A total of 28 simulation runs were performed for both zuonin A enantiomers at various poses (14 for (-)-zuonin A and 14 for (+)-zuonin A). The conditions of this step were the same as the second equilibration step except all backbone restraints were removed.

For all MD simulations a Langevin thermostat was used to regulate the system's temperature, all covalent hydrogen bond lengths were constrained using the SHAKE algorithm, and a 10Å cutoff was used for van der Waals interactions and Particle-Mesh-Ewald (PME)[18] for electrostatics.

BINDING FREE ENERGY VIA MM-GBSA

The Molecular Mechanics-Generalized Born Surface Area (MM-GBSA) method was used to calculate the free energy difference between the bound and unbound states. MD trajectories from each production run were processed with the MMPBSA.py module of Amber12. Solvation energies were calculated using the Hawkins, Cramer, Truhlar pairwise generalized Born model representation of implicit solvent. Due to the time consuming nature and unreliable methods currently available for estimating entropic contributions, it was assumed that the effect of entropy on binding was similar across all

simulations since the molecules being compared were identical and binding to similar pockets.

Chapter 3: Results and Discussion

MOLECULAR DOCKING

Molecular docking results of both zuonin enantiomers docked to the pepJIP1 binding site of JNK1 tended to cluster into two pockets that are critical for JIP1 peptide binding; the highly conserved φA-X-φB recognition site, Φ_{hyd}, and another hydrophobic pocket usually occupied by Pro158 of pepJIP1 (φA-2) or "site 2", denoted as S_2, as described by Kaoud et al., figure 8.[10] RMSD cluster analysis revealed 14 unique binding poses for each zuonin A enantiomer yielding 28 total configurations.

Of the 14 poses generated for (+)-zuonin A, 5 were bound to the Φ_{hyd} region with the tetrahydrofuran (THF) located directly in the φA-X-φB recognition site. The remaining 9 poses were localized to the S_2 region. Zuonin A's central THF ring and methyl groups occupied the same pocket as Pro158 of JIP1 in 7 of these poses while the remaining two shifted away from Arg127 and occupied the Pro158 pocket with a 1,3-benzodioxole ring.

Like (+)-zuonin A, the majority of (-)-zuonin A molecules bound to the S_2 site, 8 of 11, had the central THF ring and methyl substitutions in the vicinity of the proline pocket while the remaining three also occupied the proline pocket with a 1,3-benzodioxole ring. However, unlike (+)-zuonin A, all three poses in the Φ_{hyd} region had an elongated configuration with one 1,3-benzodioxole ring occupying the φA-X-φB recognition site with the rest of the molecule extended away from Arg127, forming interactions with a shallow groove located above the pocket.

On the whole, docking poses that aggregated in the S_2 pocket scored more favorably than those that bound to Φ_{hyd}, table 1. Decomposition of the contributions for each ligand revealed that conformations bound to S_2 had a greater contribution from lipophilic interactions than those bound to the Φ_{hyd}. The S_2 pocket is deeper in the crystal

structure than that of Φ_{hyd}, thus enhancing its ability to shield zuonin A's hydrophobic core.

Pose **20** had the highest chemscore (26.7) for (+)-zuonin A. This pose was bound to the S_2 site and had the THF ring in close proximity to the proline site with both methyl groups extended into the pocket. The pose appears to be further stabilized by the stacking of one of its 1,3-benzodioxole rings between the groove formed by Arg127, Cys163, and Asp162. This pose was quite similar to a (-)-zuonin A binding mode proposed by Kaoud et al.[11]

The highest scoring pose for (-)-zuonin A was pose **10**, table 1. This pose also interacted with the S_2 site and had a chemscore of 25.7. Unlike (+)-zuonin A, pose **10** buried one of its 1,3-benzodioxole rings into the proline pocket and extended itself in the opposite direction of Arg127 making contacts in a shallow groove in the direction of the CD domain.

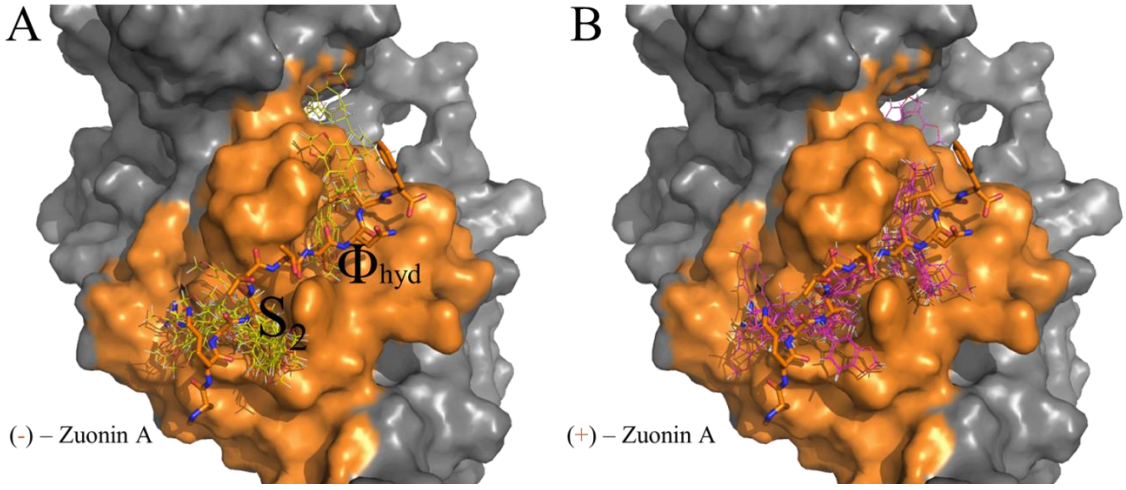

Figure 8: Docking Results for a) (-)-zuonin A and b) (+)-zuonin A. The φA-X-φB recognition site and Site 2 are denoted as Φ_{hyd} and S_2 respectively. The orange region are JNK1 atoms within an 8Å radius of each α-carbon

Table 1: JNK1/Zuonin A enantiomers docking results.

(-)Zuonin A

Pose #	ChemScore	DG	S(hbond)	S(metal)	S(lipo)	H(rot)	DE(clash)	DE(int)	Region
10	25.7	-26.3	1.29	0	169	1.28	0.42	0.15	S_2
11	24.7	-25.3	0.74	0	176	1.28	0.54	0.02	S_2
12	24.6	-24.9	0.67	0	175	1.28	0.34	0.03	S_2
27	24.2	-24.6	0.00	0	191	1.28	0.23	0.19	S_2
14	24.0	-24.5	0.46	0	178	1.28	0.22	0.29	S_2
9	24.0	-24.8	0.93	0	167	1.28	0.68	0.15	S_2
31	23.9	-24.5	0.00	0	190	1.28	0.56	0.05	S_2
24	23.8	-24.1	0.93	0	160	1.28	0.18	0.09	S_2
33	23.6	-25.7	1.80	0	149	1.28	1.83	0.24	S_2
40	23.4	-24.2	0.62	0	170	1.28	0.44	0.32	S_2
37	23.2	-23.6	0.94	0	156	1.28	0.31	0.09	S_2
43	19.6	-20.3	0.99	0	126	1.28	0.53	0.14	Φ_{hyd}
44	19.6	-20.0	0.99	0	124	1.28	0.28	0.14	Φ_{hyd}
45	18.7	-19.3	0.00	0	146	1.28	0.52	0.11	Φ_{hyd}

(+)Zuonin A

Pose #	ChemScore	DG	S(hbond)	S(metal)	S(lipo)	H(rot)	DE(clash)	DE(int)	Region
20	26.7	-27.2	1.20	0	179	1.28	0.42	0.08	S_2
1	25.5	-25.7	0.94	0	173	1.28	0.14	0.04	S_2
7	25.4	-25.6	0.92	0	174	1.28	0.18	0.00	S_2
31	24.7	-25.7	1.35	0	162	1.28	0.31	0.69	S_2
19	24.5	-24.7	0.95	0	165	1.28	0.19	0.01	S_2
22	24.3	-24.5	0.90	0	165	1.28	0.26	0.01	S_2
15	24.2	-24.5	0.90	0	165	1.28	0.23	0.08	S_2
34	23.8	-24.0	0.95	0	159	1.28	0.19	0.09	S_2
4	23.6	-23.9	0.00	0	185	1.28	0.18	0.04	S_2
41	22.3	-22.9	0.00	0	177	1.28	0.52	0.05	Φ_{hyd}
46	22.2	-22.7	0.01	0	175	1.28	0.18	0.36	Φ_{hyd}
32	21.5	-21.7	0.00	0	167	1.28	0.26	0.04	Φ_{hyd}
39	21.3	-21.9	0.00	0	168	1.28	0.12	0.48	Φ_{hyd}
49	20.8	-21.5	0.00	0	165	1.28	0.57	0.13	Φ_{hyd}

DG=Estimated binding free energy; S(hbond), S(metal), S(lipo) = hydrogen bond, metal, lipophilic contributions; H(rot) = rotatable bond contribution; DE(clash) = vdW overlap; DE(int) = internal strain; Region = docking region

MOLECULAR DYNAMICS SIMULATIONS & BINDING FREE ENERGY VIA MM-GBSA

In stark contrast to the docking scores, 8 ns molecular dynamics simulations that used the 14 unique docking configurations for each zuonin A enantiomer as a starting point revealed that zuonin A molecules bound to the φA-X-φB recognition site, Φ_{hyd}, had a lower binding free energy than those bound to the φA-2 hydrophobic pocket, S_2, for both enantiomers, table 2.

Table 2: Zuonin A/JNK1 binding free energy estimates via MM-GBSA after 8ns MD simulations. All values are in kcal/mol.

						(-)Zuonin A				
Pose #	ΔG binding	ΔG gas	ΔG solv	BOND	ANGLE	DIHED	VDWAALS	EEL	EGB	ESURF	Region
43	-26.48	-38.30	11.82	0.00	0.00	0.00	-32.93	-5.37	15.69	-3.87	Φ_{hyd}
45	-22.22	-30.77	8.55	0.00	0.00	0.00	-28.25	-2.52	12.19	-3.64	Φ_{hyd}
44	-16.72	-22.81	6.09	0.00	0.00	0.00	-23.20	0.40	8.92	-2.83	Φ_{hyd}
24	-16.21	-27.16	10.94	0.00	0.00	0.00	-22.48	-4.68	13.61	-2.66	S_2
33	-15.62	-26.67	11.05	0.00	0.00	0.00	-22.49	-4.19	13.73	-2.68	S_2
10	-15.39	-26.43	11.05	0.00	0.00	0.00	-22.36	-4.08	13.75	-2.71	S_2
9	-14.99	-25.01	10.01	0.00	0.00	0.00	-22.05	-2.96	12.66	-2.65	S_2
31	-14.30	-24.23	9.94	0.00	0.00	0.00	-20.94	-3.29	12.49	-2.56	S_2
14	-14.04	-23.66	9.62	0.00	0.00	0.00	-20.78	-2.88	12.16	-2.53	S_2
40	-13.70	-23.14	9.44	0.00	0.00	0.00	-20.30	-2.84	11.94	-2.50	S_2
37	-13.37	-20.22	6.85	0.00	0.00	0.00	-19.90	-0.32	9.26	-2.41	S_2
11	-13.29	-21.53	8.24	0.00	0.00	0.00	-19.28	-2.25	10.42	-2.18	S_2
12	-13.18	-21.91	8.73	0.00	0.00	0.00	-19.55	-2.36	11.04	-2.31	S_2
27	-12.68	-19.98	7.30	0.00	0.00	0.00	-18.93	-1.04	9.51	-2.21	S_2
						(+)Zuonin A				
Pose #	ΔG binding	ΔG gas	ΔG solv	BOND	ANGLE	DIHED	VDWAALS	EEL	EGB	ESURF	Region
39	-28.92	-38.49	9.58	0.00	0.00	0.00	-34.56	-3.93	13.68	-4.10	Φ_{hyd}
46	-27.59	-35.13	7.54	0.00	0.00	0.00	-33.37	-1.76	11.45	-3.91	Φ_{hyd}
49	-25.46	-33.03	7.57	0.00	0.00	0.00	-31.76	-1.28	11.33	-3.76	Φ_{hyd}
32	-24.20	-31.96	7.76	0.00	0.00	0.00	-30.65	-1.31	11.45	-3.69	Φ_{hyd}
41	-23.43	-35.53	12.09	0.00	0.00	0.00	-30.04	-5.49	15.74	-3.65	Φ_{hyd}
34	-16.82	-26.75	9.93	0.00	0.00	0.00	-23.98	-2.77	12.75	-2.82	S_2
1	-16.81	-27.05	10.24	0.00	0.00	0.00	-24.04	-3.01	13.08	-2.84	S_2
7	-16.66	-25.26	8.60	0.00	0.00	0.00	-24.17	-1.09	11.39	-2.79	S_2
19	-16.33	-27.20	10.87	0.00	0.00	0.00	-23.12	-4.07	13.56	-2.69	S_2
31	-16.20	-25.11	8.90	0.00	0.00	0.00	-21.98	-3.13	11.41	-2.50	S_2
20	-15.77	-25.04	9.27	0.00	0.00	0.00	-22.61	-2.43	11.99	-2.72	S_2
15	-15.33	-25.75	10.42	0.00	0.00	0.00	-21.96	-3.79	13.06	-2.63	S_2
4	-15.23	-24.62	9.39	0.00	0.00	0.00	-22.31	-2.30	11.96	-2.57	S_2
22	-14.28	-21.82	7.54	0.00	0.00	0.00	-19.75	-2.08	9.87	-2.33	S_2

ΔGbinding, ΔGgas, ΔGsolv = solvated binding free energy, binding free energy in vacuum, solvation free energy; BOND, ANGLE, DIHED = bond length, bond angle, dihedral angle energies; VDWAALS, EEL = vdW interactions and electrostatics energies; EGB, ESURF = polar and nonpolar solvation energies

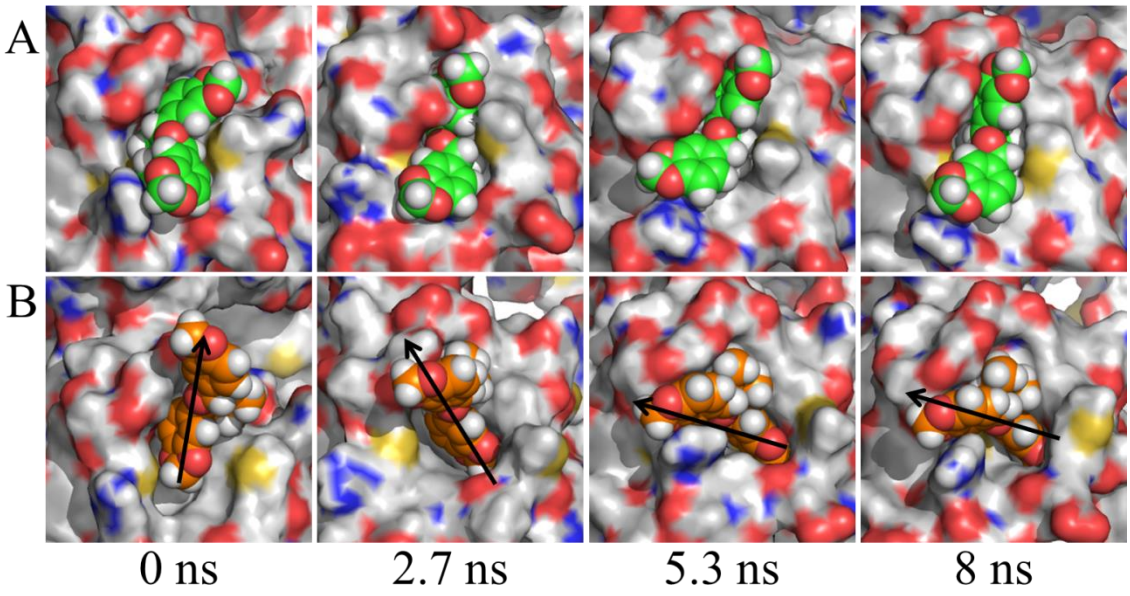

Figure 9: Trajectory of the "tightest" binding poses, as determined by MM-GBSA calculations, for A) (+)-zuonin A pose **39**, green, and B) (-)-zuonin A pose **43**, orange, with a vector to emphasize the change in orientation. Both are bound to Φ_{hyd} binding site.

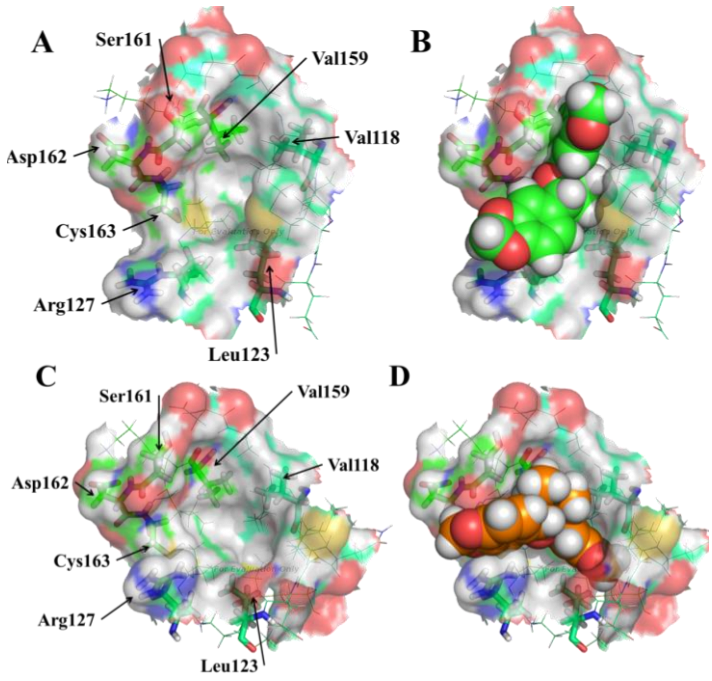

Figure 10: Stable binding pose of a) (-)-Zuonin A pose **43** and b) (+)-Zuonin A pose **39**. Enlarged as Figure S11

Over the course of the MD simulation, the docking prediction pose **43** for (-)-zuonin A assumed a stable conformation with the tetrahydrofuran ring occupying the φA site normally occupied by Leu159 of JIP1. Both methyl groups were on the solvent facing side of the ring in the vicinity of the φB recognition site. Visualization of pose **43**'s MD trajectory showed that several key movements were necessary to achieve this thermodynamically favorable binding mode, figure 9. At the beginning of the simulation, one of (-)-zuonin A's 1,3-benzodioxole rings is originally bound to the φA-X-φB recognition site. Rotation of (-)-zuonin A occurs when the upper 1,3-benzodioxole ring begins to slide past the residues Val159, Lys160, Ser161 and Asp162 which create the upper portion of the pocket. Simultaneously, Glu117-Leu123 undergo a movement in their backbone which creates an induced fit hydrophobic pocket available for tighter binding of the second 1,3-benzodioxole ring. The (-)-zuonin A molecule then gets "locked" into place as Arg127 swings upward toward the first 1,3-benzodioxole ring and holds it between its guanidinium cap and the backbone of Asp162 using the side chain of Cys163 as a base.

Decomposing the binding free energy into the contributions from each JNK amino acid reveals several significant interactions, table 3. One interaction involves the side chain of Val118, -1.787 kcal/mol, which appears to wedge itself between one of (-)-zuonin A's methyls and the 1,3-benzodioxole ring bound to the induced hydrophobic pocket, figures 10c & 10d. A similar interaction occurs between the backbone of Ser161, -1.361 kcal/mol, and the other side of the THF ring. The residues involved in immobilizing the other 1,3-benzodioxole ring, Arg127, Asp162, and Cys163, all provide major contributions to (-)-zuonin A binding with binding free energies of -1.623, -1.026, and -1.243 kcal/mol respectively. Other contributions come from the hydrophobic amino

acids that line the inside of both the φA-X-φB recognition site in addition to those that line the induced hydrophobic pocket, table 3.

Table 3: Free energy contributions of JNK1 residues to the binding of (-)-zuonin A once it has assumed its stable conformation (4-8ns). Complete data available in STable14-STable16

Free Energy Decomposition of (-)-Zuonin A binding

	Side Chain + Backbone Energies						Side Chain	Backbone
Residue	TOTAL	Internal	vdW	Electro-statics	Polar Solv.	Non-Polar Solv.	TOTAL	TOTAL
VAL118	-1.787	0.000	-1.719	-0.395	0.563	-0.237	-1.502	-0.286
ARG127	-1.623	0.000	-2.168	-3.704	4.632	-0.384	-1.583	-0.041
LEU123	-1.452	0.000	-1.364	-0.211	0.296	-0.173	-1.332	-0.119
SER161	-1.361	0.000	-2.130	-0.346	1.476	-0.361	-0.148	-1.213
VAL159	-1.258	0.000	-1.405	0.182	0.079	-0.114	-1.073	-0.186
CYS163	-1.243	0.000	-1.514	0.267	0.135	-0.131	-0.737	-0.505
ASP162	-1.026	0.000	-1.120	-0.183	0.364	-0.086	-0.081	-0.945
LEU131	-1.008	0.000	-0.970	-0.106	0.152	-0.083	-0.959	-0.049
MET121	-0.900	0.000	-0.897	-0.690	0.758	-0.071	-0.439	-0.461
LYS160	-0.897	0.000	-1.055	0.072	0.143	-0.056	-0.018	-0.879
ILE119	-0.845	0.000	-0.864	-0.380	0.427	-0.027	-0.265	-0.580
LEU115	-0.652	0.000	-0.645	0.062	-0.044	-0.024	-0.516	-0.135

The binding free energies calculated for the various (+)-zuonin A trajectories suggests that the (+)-zuonin A enantiomer may also prefer binding to the φA-X-φB recognition site, but in a different fashion. The two poses with the lowest binding energy for (+)-zuonin A were **39** and **46** both adopted very similar binding modes. The THF ring still primarily occupies the φA site, however, unlike with (-)-zuonin A, the two methyl groups point in toward the hydrophobic core and create a small hydrophobic pocket in the same location as the one occupied in the (-)-zuonin A model. Unlike, (-)-zuonin A's more dynamic movement, (+)-zuonin A pose **39** stays relatively stationary except for a noticeable dynamic movement of Arg127's side chain which swings down and away

from the 1,3-benzodioxole ring of (+)-zuonin A, giving the ring space to lay flat on the peptide backbone of Cys163, figures 10a & b.

The large movement of (-)-zuonin A in the Φ_{hyd} pocket caused it to have a larger standard deviation in its binding free energy (~6 kcal/mol) compared to the other studied poses (~2 kcal/mol), Stable 8. The binding free energy of poses **43** for (-)-zuonin A and **39** for (+)-zuonin A in their most stable states (4-8ns) showed that indeed (-)-zuonin A (-32 kcal/mol) bound to JNK1 with a slightly lower binding free energy than (+)-zuonin A (-30 kcal/mol), Stable 13.

It is to be noted that entropy contributions are not included in these free energy values since current calculation methods are typically time consuming and unreliable. Therefore, the free energy values as presented here represent binding enthalpy and changes in enthalpy during solvation.

COMPARISON TO PREVIOUS (-)-ZUONIN A BINDING MODEL

Lastly, it is important to address a previous (-)-zuonin A/JNK interaction study performed by Yan et al.[11] which proposed a model of (-)-zuonin binding where the inhibitor was bound to the S_2 region of JNK. Residues that were considered important for (-)-zuonin A binding to the S_2 site were mutated to alanines and kinetic/inhibition assays were performed on the mutants. Of the 5 mutants made (R127A, T164A, W324A, Y130A, C163A) only the R127A mutant led to altered kinetic parameters for c-Jun phosphorylation in the absence of (-)-zuonin A. This data further supports R127's significance in substrate/ligand recognition.

Table 4: (-)-Zuonin A inhibition data for JNK mutants published by Kaoud et al.[11] K_m k_{cat} and k_{cat}/K_m describe the binding and phosphorylation of c-Jun by JNK2. IC50 and % inhibition describe the (-)-zuonin A concentration necessary to achieve 50% of the maximal inhibition and the maximal percentage of inhibition compared to the baseline at saturating concentrations.

Mutants	K_m **(μM)**	k_{cat} **(s^{-1})**	k_{cat}/K_m **(μM s^{-1})**	**IC50(μM)**	**% inhibition at 200 μM**
JNK2 *WT*	1.65 ± 0.1	1 ± 0.15	0.6	2.9 ± 0.17	70
JNK2 (R127A)	23.6 ± 1.1	1.4 ± 0.3	0.06	14 ± 2.1	80
JNK2 (Y130A)	1.87 ± 0.3	1 ± 0.04	0.53	2.3 ± 0.16	95
JNK2 (C163A)	1.33 ± 0.4	1 ± 0.065	0.75	37 ± 2.5	37
JNK2 (T164A)	0.73 ± 0.18	1.1 ± 0.064	1.5	13.6 ± 1.5	39
JNK2 (W324A)	2.3 ± 0.15	1.06 ± 0.075	0.46	16.6 ± 0.17	98
JNK2 (D326A)	2 ± 0.83	0.8 ± 0.08	0.4	2.8 ± 0.32	71

Mutants R127A, C163A and T164A are common to both the S_2 binding pocket and the Φ_{hyd} pocket and provide important binding interactions in both models. The perturbed binding of c-Jun by the R127A mutant makes it difficult to derive any conclusions regarding inhibitor binding, however the IC_{50} values for mutants C163A and T164A both increased by over 1100% and 360% respectively while their maximal inhibition was nearly halved clearly showing that these mutations have some effect on inhibitor binding which would be expected in either model, table 4.

An interesting discovery from the previous study was that mutations of the large side chain amino acids Y130 and W324 to alanine in the S_2 binding pocket did not alter c-Jun binding, but increased the percentage inhibition of (-)-zuonin A from 70% when complexed with wild type JNK2 to 95% and 98% when bound to the mutants Y130A and W324A. Although this result does support the possibility that (-)-zuonin A does indeed bind to the S_2 pocket, one must also consider the effects that these large mutations had on the S_2 binding region.

It is not out of the realm of possibility that (-)-zuonin A could sample both the S_2 and Φ_{hyd} pocket of WT JNK2, but based on simulation data, may prefer binding to the latter. This conformation may be the tightest fit for (-)-zuonin A but its binding mode may only inhibit 70% of the reactions that occur. Expanding the S_2 binding pocket by mutating Y130 and W324 to alanine may increase the probability of (-)-zuonin A binding to that region where it can more effectively block c-Jun binding either in a singular fashion or by binding to both S_2 and Φ_{hyd} pockets.

In order to gain further insight and validation into the Φ_{hyd} binding model, it would be beneficial to mutate JNK residues that are predicted to contribute the most to (-)-zuonin binding based on MD simulation data and are unique to the Φ_{hyd} region, such as Val118, Leu123, and Val 159.

Chapter 4: Conclusions

Previous work has shown that enantiomers (+)-zuonin A and & (-)-zuonin A can bind to different JNK isoforms with a high specificity over other MAP kinases and disrupt JNK/substrate interactions at the D-recruitment site (DRS). Although they have a similar affinity for JNK, (-)-zuonin A inhibits 80% of JNK phosphorylation events, while (+)-zuonin A only inhibits 15% at saturated levels.

In this study, molecular docking and molecular dynamics simulations were utilized to examine binding interactions between JNK and both zuonin A enantiomers and to identify differences in their binding modes. First, a series of potential binding pockets and poses were determined using molecular docking experiments along the DRS using the JNK1-pepJIP1 crystal structure as a guide. Each pose was then subjected to molecular dynamics simulations to account for explicit solvent effects and dynamic interactions within the system. The trajectories were then used to estimate the binding free energy for each pose in hopes of discovering the most likely binding interaction.

The results support the limitation of docking only experiments which allow for free movement of the ligand, but rely heavily on a rigid target structure. MD simulation results showed that JNK can alter its structure in the presence of either zuonin enantiomer in order to better accommodate binding of the inhibitor.

Although the results of both simulations have both zuonin A enantiomers binding in the same Φ_{hyd} region of JNK1's DRS, they adopt different conformations and have different levels of thermodynamic stability. This difference in thermodynamic stability may explain why (-)-zuonin A's increased effectiveness at inhibiting the phosphorylation of JNK's substrates over (+)-zuonin A.

In addition, the proposed Φ_{hyd} (-)-zuonin A binding model was determined using a different method than that used to describe a previous binding model which suggests (-)-zuonin A binds to the S_2 binding region. It is possible that these models are not mutually exclusive, but could work in conjunction with one another. To gain a better insight, it would be beneficial to physically mutate residues that are unique to the Φ_{hyd} pocket and predicted to contribute the largest binding interactions for (-)-zuonin A and note any changes in the effectiveness of zuonin A binding and inhibition.

Appendix

STable 5: Total free energy and decomposition of contributions for each (-)-zuonin A/JNK1 complex used in (-)-zuonin A binding free energy calculations

(-)-Zuonin A/JNK1 Complex

	BOND			ANGLE			DIHED			VDWAALS		
Pose #	Avg	Std. Dev.	Std. Err. of Mean	Avg	Std. Dev.	Std. Err. of Mean	Avg	Std. Dev.	Std. Err. of Mean	Avg	Std. Dev.	Std. Err. of Mean
9	1116.87	28.63	1.01	3060.12	40.39	1.43	3834.89	23.46	0.83	-2854.83	24.81	0.88
10	1116.32	28.26	1.00	3044.67	41.66	1.47	3833.11	26.16	0.92	-2849.52	23.52	0.83
11	1115.35	27.72	0.98	3057.73	43.01	1.52	3829.32	24.93	0.88	-2845.69	23.36	0.83
12	1117.25	27.82	0.98	3058.82	42.55	1.50	3833.13	26.26	0.93	-2871.83	29.37	1.04
14	1115.32	28.42	1.00	3048.20	42.37	1.50	3827.03	25.91	0.92	-2853.19	24.20	0.86
24	1115.58	27.13	0.96	3055.55	42.54	1.50	3827.71	23.69	0.84	-2854.35	33.21	1.17
27	1116.51	28.44	1.01	3053.99	42.47	1.50	3837.28	25.15	0.89	-2844.92	26.03	0.92
31	1115.00	28.72	1.02	3044.72	41.32	1.46	3837.95	24.06	0.85	-2851.73	27.74	0.98
33	1113.09	28.37	1.00	3053.08	42.81	1.51	3830.55	24.88	0.88	-2850.82	26.72	0.94
37	1115.70	28.45	1.01	3059.60	42.30	1.50	3827.67	26.09	0.92	-2845.98	26.05	0.92
40	1114.22	28.12	0.99	3057.44	42.22	1.49	3829.82	25.14	0.89	-2852.76	27.63	0.98
43	1116.83	28.65	1.01	3058.74	43.69	1.54	3828.86	24.60	0.87	-2872.18	26.78	0.95
44	1117.80	28.72	1.02	3062.70	42.43	1.50	3836.09	26.20	0.93	-2865.94	31.89	1.13
45	1116.31	29.57	1.05	3059.85	41.44	1.47	3826.05	23.82	0.84	-2859.54	27.06	0.96

	EEL			EGB			ESURF		
Pose #	Avg	Std. Dev.	Std. Err. of Mean	Avg	Std. Dev.	Std. Err. of Mean	Avg	Std. Dev.	Std. Err. of Mean
9	-26160.93	150.73	5.33	-4589.06	122.35	4.33	134.05	2.42	0.09
10	-26114.98	98.33	3.48	-4620.97	79.10	2.80	135.95	1.84	0.07
11	-26014.34	154.11	5.45	-4714.22	119.42	4.22	137.42	2.08	0.07
12	-25989.07	101.29	3.58	-4684.78	85.23	3.01	133.43	2.27	0.08
14	-26087.91	134.51	4.76	-4605.07	98.04	3.47	135.34	2.11	0.07
24	-26036.06	180.48	6.38	-4703.65	136.60	4.83	137.18	3.35	0.12
27	-26075.19	137.20	4.85	-4660.65	132.13	4.67	136.67	2.18	0.08
31	-26058.48	92.15	3.26	-4658.85	74.93	2.65	137.46	2.64	0.09
33	-26034.71	135.47	4.79	-4693.68	104.51	3.69	134.98	2.53	0.09
37	-25944.50	104.86	3.71	-4768.40	80.88	2.86	136.54	2.17	0.08
40	-26098.86	106.08	3.75	-4636.00	78.89	2.79	134.82	2.36	0.08
43	-26028.17	168.35	5.95	-4697.32	112.12	3.96	133.29	2.85	0.10
44	-25884.75	133.68	4.73	-4780.74	115.73	4.09	134.92	3.09	0.11
45	-26130.72	160.58	5.68	-4563.82	120.13	4.25	132.63	2.18	0.08

	G gas			G solv			TOTAL		
Pose #	Avg	Std. Dev.	Std. Err. of Mean	Avg	Std. Dev.	Std. Err. of Mean	Avg	Std. Dev.	Std. Err. of Mean
9	-21003.87	162.28	5.74	-4455.02	122.38	4.33	-25458.89	56.69	2.00
10	-20970.41	115.94	4.10	-4485.01	79.12	2.80	-25455.42	54.50	1.93
11	-20857.63	165.94	5.87	-4576.81	119.44	4.22	-25434.44	61.19	2.16
12	-20851.70	119.99	4.24	-4551.35	85.26	3.01	-25403.05	58.93	2.08
14	-20950.55	148.17	5.24	-4469.73	98.06	3.47	-25420.29	57.54	2.03
24	-20891.57	191.79	6.78	-4566.47	136.64	4.83	-25458.04	63.15	2.23
27	-20912.34	150.82	5.33	-4523.98	132.15	4.67	-25436.32	57.21	2.02
31	-20912.55	111.23	3.93	-4521.39	74.98	2.65	-25433.94	61.58	2.18
33	-20888.81	149.41	5.28	-4558.70	104.54	3.70	-25447.51	63.82	2.26
37	-20787.51	122.28	4.32	-4631.86	80.91	2.86	-25419.37	57.15	2.02
40	-20950.16	123.37	4.36	-4501.18	78.93	2.79	-25451.34	59.04	2.09
43	-20895.93	179.98	6.36	-4564.04	112.16	3.97	-25459.97	62.91	2.22
44	-20734.11	148.99	5.27	-4645.81	115.77	4.09	-25379.92	60.49	2.14
45	-20988.05	172.27	6.09	-4431.19	120.15	4.25	-25419.24	64.12	2.27

STable 6: Total free energy and decomposition of contributions of the receptor, JNK1, used in (-)-zuonin A binding free energy calculations

JNK1 (Receptor)

	BOND			ANGLE			DIHED			VDWAALS		
Pose #	Avg	Std. Dev.	Std. Err. of Mean	Avg	Std. Dev.	Std. Err. of Mean	Avg	Std. Dev.	Std. Err. of Mean	Avg	Std. Dev.	Std. Err. of Mean
9	1105.25	28.38	1.00	3012.26	40.18	1.42	3811.43	23.48	0.83	-2829.38	24.99	0.88
10	1104.70	28.12	0.99	2997.11	41.58	1.47	3809.88	25.94	0.92	-2823.72	23.45	0.83
11	1103.90	27.67	0.98	3009.46	42.97	1.52	3806.46	24.98	0.88	-2822.78	23.61	0.83
12	1105.65	27.74	0.98	3010.77	42.44	1.50	3809.79	26.02	0.92	-2848.87	29.47	1.04
14	1103.80	28.21	1.00	3000.22	42.17	1.49	3803.75	25.91	0.92	-2829.07	24.09	0.85
24	1104.18	26.97	0.95	3007.80	42.55	1.50	3804.07	23.72	0.84	-2828.34	33.07	1.17
27	1104.95	28.24	1.00	3005.98	42.27	1.49	3813.57	24.98	0.88	-2822.50	25.68	0.91
31	1103.60	28.49	1.01	2996.65	41.20	1.46	3814.75	24.05	0.85	-2827.23	27.19	0.96
33	1101.66	28.10	0.99	3005.35	42.77	1.51	3807.31	24.87	0.88	-2824.92	26.39	0.93
37	1104.15	28.38	1.00	3011.91	42.09	1.49	3804.30	25.93	0.92	-2822.70	25.94	0.92
40	1102.80	28.05	0.99	3009.72	42.06	1.49	3806.57	25.07	0.89	-2829.14	27.92	0.99
43	1105.44	28.42	1.01	3010.93	43.44	1.54	3805.51	24.49	0.87	-2835.54	25.21	0.89
44	1106.34	28.62	1.01	3014.58	42.20	1.49	3812.81	26.04	0.92	-2839.24	32.21	1.14
45	1104.71	29.53	1.04	3011.56	41.26	1.46	3803.12	23.53	0.83	-2827.80	27.07	0.96

	EEL			EGB			ESURF		
Pose #	Avg	Std. Dev.	Std. Err. of Mean	Avg	Std. Dev.	Std. Err. of Mean	Avg	Std. Dev.	Std. Err. of Mean
9	-26058.73	150.79	5.33	-4586.80	123.05	4.35	133.91	2.48	0.09
10	-26010.73	98.66	3.49	-4620.65	79.28	2.80	135.87	1.83	0.06
11	-25910.55	153.15	5.41	-4710.16	119.72	4.23	136.80	2.12	0.07
12	-25889.16	101.27	3.58	-4681.21	84.81	3.00	132.96	2.30	0.08
14	-25985.58	134.37	4.75	-4602.56	98.07	3.47	135.09	2.10	0.07
24	-25931.59	179.85	6.36	-4702.26	136.51	4.83	137.06	3.35	0.12
27	-25974.06	137.48	4.86	-4655.20	132.14	4.67	136.10	2.13	0.08
31	-25952.55	91.89	3.25	-4656.86	75.13	2.66	137.23	2.64	0.09
33	-25929.34	136.58	4.83	-4693.11	104.45	3.69	134.87	2.52	0.09
37	-25846.42	104.84	3.71	-4762.80	80.97	2.86	136.17	2.16	0.08
40	-25995.89	105.90	3.74	-4633.11	79.25	2.80	134.54	2.41	0.09
43	-25919.34	166.06	5.87	-4698.30	109.36	3.87	134.37	2.48	0.09
44	-25786.00	134.18	4.74	-4774.93	115.98	4.10	134.97	3.20	0.11
45	-26029.28	159.50	5.64	-4561.35	120.08	4.25	133.49	2.23	0.08

	G gas			G solv			TOTAL		
Pose #	Avg	Std. Dev.	Std. Err. of Mean	Avg	Std. Dev.	Std. Err. of Mean	Avg	Std. Dev.	Std. Err. of Mean
9	-20959.17	162.28	5.74	-4452.89	123.08	4.35	-25412.06	56.20	1.99
10	-20922.76	116.09	4.10	-4484.77	79.30	2.80	-25407.54	54.19	1.92
11	-20813.50	165.07	5.84	-4573.35	119.74	4.23	-25386.86	61.36	2.17
12	-20811.81	119.88	4.24	-4548.24	84.84	3.00	-25360.06	58.66	2.07
14	-20906.87	147.93	5.23	-4467.47	98.09	3.47	-25374.34	57.40	2.03
24	-20843.88	191.15	6.76	-4565.20	136.55	4.83	-25409.07	63.02	2.23
27	-20872.06	150.89	5.33	-4519.10	132.15	4.67	-25391.16	56.58	2.00
31	-20864.77	110.77	3.92	-4519.63	75.18	2.66	-25384.41	61.17	2.16
33	-20839.95	150.29	5.31	-4558.24	104.48	3.69	-25398.18	63.42	2.24
37	-20748.76	122.12	4.32	-4626.64	81.00	2.86	-25375.40	56.88	2.01
40	-20905.94	123.20	4.36	-4498.56	79.29	2.80	-25404.50	59.05	2.09
43	-20833.01	177.50	6.28	-4563.93	109.38	3.87	-25396.93	60.54	2.14
44	-20691.52	149.40	5.28	-4639.96	116.02	4.10	-25331.48	60.44	2.14
45	-20937.69	171.18	6.05	-4427.86	120.10	4.25	-25365.56	64.44	2.28

STable 7: Total free energy and decomposition of contributions of the ligand, (-)-zuonin A, used in (-)-zuonin A binding free energy calculations

(-)-Zuonin A (Ligand)

	BOND			ANGLE			DIHED			VDWAALS		
Pose #	Avg	Std. Dev.	Std. Err. of Mean	Avg	Std. Dev.	Std. Err. of Mean	Avg	Std. Dev.	Std. Err. of Mean	Avg	Std. Dev.	Std. Err. of Mean
9	11.62	2.91	0.10	47.86	3.65	0.13	23.47	2.31	0.08	-3.40	1.00	0.04
10	11.62	2.87	0.10	47.56	3.89	0.14	23.23	2.36	0.08	-3.45	0.96	0.03
11	11.44	2.79	0.10	48.27	3.66	0.13	22.86	2.22	0.08	-3.63	0.95	0.03
12	11.59	2.83	0.10	48.06	3.76	0.13	23.34	2.27	0.08	-3.41	0.95	0.03
14	11.52	2.79	0.10	47.97	3.63	0.13	23.27	2.34	0.08	-3.34	1.03	0.04
24	11.39	2.70	0.10	47.75	4.02	0.14	23.64	2.30	0.08	-3.54	0.91	0.03
27	11.56	3.01	0.11	48.01	3.85	0.14	23.71	2.61	0.09	-3.49	0.97	0.03
31	11.39	2.96	0.10	48.07	3.69	0.13	23.19	2.42	0.09	-3.55	0.93	0.03
33	11.43	2.80	0.10	47.73	3.96	0.14	23.23	2.38	0.08	-3.41	0.97	0.03
37	11.55	2.90	0.10	47.68	3.72	0.13	23.37	2.34	0.08	-3.37	0.94	0.03
40	11.41	2.92	0.10	47.72	3.76	0.13	23.25	2.23	0.08	-3.33	0.97	0.03
43	11.39	2.85	0.10	47.81	3.76	0.13	23.35	2.28	0.08	-3.71	0.85	0.03
44	11.46	2.84	0.10	48.12	3.95	0.14	23.28	2.29	0.08	-3.49	0.98	0.03
45	11.60	2.98	0.11	48.29	3.74	0.13	22.93	2.24	0.08	-3.49	0.99	0.03

	EEL			EGB			ESURF		
Pose #	Avg	Std. Dev.	Std. Err. of Mean	Avg	Std. Dev.	Std. Err. of Mean	Avg	Std. Dev.	Std. Err. of Mean
9	-99.24	1.86	0.07	-14.92	0.64	0.02	2.78	0.03	0.00
10	-100.17	1.71	0.06	-14.07	0.63	0.02	2.79	0.02	0.00
11	-101.54	2.72	0.10	-14.48	0.63	0.02	2.79	0.02	0.00
12	-97.55	2.05	0.07	-14.62	0.64	0.02	2.78	0.02	0.00
14	-99.46	2.30	0.08	-14.67	0.62	0.02	2.78	0.02	0.00
24	-99.79	1.78	0.06	-14.99	0.53	0.02	2.78	0.02	0.00
27	-100.09	1.80	0.06	-14.95	0.48	0.02	2.78	0.03	0.00
31	-102.65	2.85	0.10	-14.48	0.58	0.02	2.79	0.02	0.00
33	-101.18	2.42	0.09	-14.30	0.67	0.02	2.78	0.02	0.00
37	-97.76	2.40	0.08	-14.86	0.56	0.02	2.78	0.02	0.00
40	-100.14	2.24	0.08	-14.84	0.52	0.02	2.78	0.02	0.00
43	-103.47	1.80	0.06	-14.71	0.47	0.02	2.78	0.02	0.00
44	-99.14	2.19	0.08	-14.73	0.64	0.02	2.78	0.02	0.00
45	-98.93	2.62	0.09	-14.67	0.64	0.02	2.79	0.02	0.00

	G gas			G solv			TOTAL		
Pose #	Avg	Std. Dev.	Std. Err. of Mean	Avg	Std. Dev.	Std. Err. of Mean	Avg	Std. Dev.	Std. Err. of Mean
9	-19.70	5.62	0.20	-12.14	0.64	0.02	-31.84	4.47	0.16
10	-21.21	5.73	0.20	-11.29	0.63	0.02	-32.49	4.67	0.17
11	-22.60	5.87	0.21	-11.70	0.63	0.02	-34.29	4.52	0.16
12	-17.98	5.70	0.20	-11.84	0.64	0.02	-29.82	4.65	0.16
14	-20.02	5.73	0.20	-11.89	0.62	0.02	-31.91	4.65	0.16
24	-20.54	5.72	0.20	-12.21	0.53	0.02	-32.76	4.57	0.16
27	-20.31	5.90	0.21	-12.17	0.48	0.02	-32.48	4.90	0.17
31	-23.54	6.10	0.22	-11.70	0.58	0.02	-35.24	4.78	0.17
33	-22.19	5.99	0.21	-11.52	0.67	0.02	-33.71	4.49	0.16
37	-18.53	5.86	0.21	-12.08	0.56	0.02	-30.60	4.58	0.16
40	-21.08	5.80	0.21	-12.06	0.53	0.02	-33.14	4.66	0.16
43	-24.63	5.60	0.20	-11.93	0.47	0.02	-36.55	4.62	0.16
44	-19.77	5.88	0.21	-11.95	0.64	0.02	-31.72	4.76	0.17
45	-19.59	5.98	0.21	-11.88	0.64	0.02	-31.47	4.74	0.17

STable 8: Binding free energy of (-)-zuonin A to JNK1 calculated by taking the difference of Complex-Receptor-Ligand

Difference (Complex - Receptor - Ligand) [(-)-Zuonin A/JNK1]

	BOND			ANGLE			DIHED			VDWAALS		
Pose #	Avg	Std. Dev.	Std. Err. of Mean	Avg	Std. Dev.	Std. Err. of Mean	Avg	Std. Dev.	Std. Err. of Mean	Avg	Std. Dev.	Std. Err. of Mean
9	0.00	0.00	0.00	0.00	0.00	0.00	0.00	0.01	0.00	-22.05	2.85	0.10
10	0.00	0.00	0.00	0.00	0.00	0.00	0.00	0.01	0.00	-22.36	2.07	0.07
11	0.00	0.00	0.00	0.00	0.00	0.00	0.00	0.01	0.00	-19.28	3.08	0.11
12	0.00	0.00	0.00	0.00	0.00	0.00	0.00	0.01	0.00	-19.55	2.65	0.09
14	0.00	0.00	0.00	0.00	0.00	0.00	0.00	0.01	0.00	-20.78	2.38	0.08
24	0.00	0.00	0.00	0.00	0.00	0.00	0.00	0.01	0.00	-22.48	2.43	0.09
27	0.00	0.00	0.00	0.00	0.00	0.00	0.00	0.01	0.00	-18.93	2.59	0.09
31	0.00	0.00	0.00	0.00	0.00	0.00	0.00	0.01	0.00	-20.94	2.67	0.09
33	0.00	0.00	0.00	0.00	0.00	0.00	0.00	0.01	0.00	-22.49	2.57	0.09
37	0.00	0.00	0.00	0.00	0.00	0.00	0.00	0.01	0.00	-19.90	2.45	0.09
40	0.00	0.00	0.00	0.00	0.00	0.00	0.00	0.01	0.00	-20.30	2.26	0.08
43	0.00	0.00	0.00	0.00	0.00	0.00	0.00	0.01	0.00	-32.93	6.86	0.24
44	0.00	0.00	0.00	0.00	0.00	0.00	0.00	0.01	0.00	-23.20	3.12	0.11
45	0.00	0.00	0.00	0.00	0.00	0.00	0.00	0.01	0.00	-28.25	2.88	0.10

	EEL			EGB			ESURF		
Pose #	Avg	Std. Dev.	Std. Err. of Mean	Avg	Std. Dev.	Std. Err. of Mean	Avg	Std. Dev.	Std. Err. of Mean
9	-2.96	3.20	0.11	12.66	3.50	0.12	-2.65	0.30	0.01
10	-4.08	1.99	0.07	13.75	2.12	0.08	-2.71	0.20	0.01
11	-2.25	2.09	0.07	10.42	2.06	0.07	-2.18	0.37	0.01
12	-2.36	2.01	0.07	11.04	2.18	0.08	-2.31	0.30	0.01
14	-2.88	1.91	0.07	12.16	1.99	0.07	-2.53	0.24	0.01
24	-4.68	2.39	0.08	13.61	2.55	0.09	-2.66	0.23	0.01
27	-1.04	2.57	0.09	9.51	2.33	0.08	-2.21	0.26	0.01
31	-3.29	2.73	0.10	12.49	2.64	0.09	-2.56	0.29	0.01
33	-4.19	2.07	0.07	13.73	2.26	0.08	-2.68	0.27	0.01
37	-0.32	2.67	0.09	9.26	2.19	0.08	-2.41	0.27	0.01
40	-2.84	2.13	0.08	11.94	2.40	0.09	-2.50	0.25	0.01
43	-5.37	3.81	0.13	15.69	4.65	0.16	-3.87	0.70	0.02
44	0.40	2.77	0.10	8.92	2.25	0.08	-2.83	0.42	0.01
45	-2.52	2.09	0.07	12.19	1.89	0.07	-3.64	0.36	0.01

	ΔG gas			ΔG solv			ΔG binding		
Pose #	Avg	Std. Dev.	Std. Err. of Mean	Avg	Std. Dev.	Std. Err. of Mean	Avg	Std. Dev.	Std. Err. of Mean
9	-25.01	4.29	0.15	10.01	3.51	0.12	-14.99	2.41	0.09
10	-26.43	2.87	0.10	11.05	2.13	0.08	-15.39	1.88	0.07
11	-21.53	3.72	0.13	8.24	2.09	0.07	-13.29	2.67	0.09
12	-21.91	3.32	0.12	8.73	2.20	0.08	-13.18	2.02	0.07
14	-23.66	3.05	0.11	9.62	2.00	0.07	-14.04	1.96	0.07
24	-27.16	3.41	0.12	10.94	2.56	0.09	-16.21	2.02	0.07
27	-19.98	3.65	0.13	7.30	2.35	0.08	-12.68	2.31	0.08
31	-24.23	3.82	0.14	9.94	2.66	0.09	-14.30	2.19	0.08
33	-26.67	3.30	0.12	11.05	2.27	0.08	-15.62	2.28	0.08
37	-20.22	3.62	0.13	6.85	2.21	0.08	-13.37	1.87	0.07
40	-23.14	3.10	0.11	9.44	2.42	0.09	-13.70	1.78	0.06
43	-38.30	7.84	0.28	11.82	4.71	0.17	-26.48	6.36	0.22
44	-22.81	4.17	0.15	6.09	2.29	0.08	-16.72	2.53	0.09
45	-30.77	3.55	0.13	8.55	1.93	0.07	-22.22	2.84	0.10

STable 9: Total free energy and decomposition of contributions for each (+)-zuonin A/JNK1 complex used in (+)-zuonin A binding free energy calculations

(+)-Zuonin A/JNK1 Complex

Pose #	BOND			ANGLE			DIHED			VDWAALS		
	Avg	Std. Dev.	Std. Err. of Mean	Avg	Std. Dev.	Std. Err. of Mean	Avg	Std. Dev.	Std. Err. of Mean	Avg	Std. Dev.	Std. Err. of Mean
1	1113.88	28.48	1.01	3057.08	42.19	1.49	3831.70	26.32	0.93	-2878.97	26.79	0.95
4	1115.19	28.02	0.99	3052.19	43.67	1.54	3831.22	26.26	0.93	-2845.69	28.69	1.01
7	1115.30	27.91	0.99	3065.93	42.10	1.49	3838.74	25.71	0.91	-2869.92	25.13	0.89
15	1116.19	28.77	1.02	3059.38	40.66	1.44	3833.36	25.37	0.90	-2861.33	28.68	1.01
19	1115.71	27.58	0.98	3056.93	43.52	1.54	3829.07	24.68	0.87	-2878.89	28.52	1.01
20	1117.37	28.68	1.01	3057.94	41.02	1.45	3825.86	25.10	0.89	-2836.37	23.39	0.83
22	1117.11	29.88	1.06	3057.99	41.39	1.46	3831.70	24.77	0.88	-2852.73	27.04	0.96
31	1112.81	29.32	1.04	3045.51	42.56	1.50	3838.84	24.57	0.87	-2869.71	24.65	0.87
32	1117.05	27.94	0.99	3058.64	42.60	1.51	3823.75	26.58	0.94	-2860.23	27.92	0.99
34	1118.73	28.04	0.99	3059.41	42.76	1.51	3811.32	26.61	0.94	-2831.49	30.35	1.07
39	1115.96	27.04	0.96	3052.43	41.85	1.48	3834.32	23.57	0.83	-2897.22	27.83	0.98
41	1112.78	27.46	0.97	3049.85	42.81	1.51	3838.48	23.65	0.84	-2876.38	25.64	0.91
46	1116.29	28.89	1.02	3055.28	42.26	1.49	3838.88	27.17	0.96	-2866.88	23.31	0.82
49	1115.35	27.80	0.98	3050.82	40.48	1.43	3837.95	25.33	0.90	-2876.36	35.19	1.24

Pose #	EEL			EGB			ESURF		
	Avg	Std. Dev.	Std. Err. of Mean	Avg	Std. Dev.	Std. Err. of Mean	Avg	Std. Dev.	Std. Err. of Mean
1	-26187.02	107.09	3.79	-4550.76	91.00	3.22	131.50	2.86	0.10
4	-26024.35	163.50	5.78	-4692.13	117.26	4.15	136.17	2.48	0.09
7	-26278.14	138.35	4.89	-4479.34	99.17	3.51	130.35	2.36	0.08
15	-26003.99	102.74	3.63	-4702.27	96.58	3.41	133.88	2.55	0.09
19	-26111.23	129.89	4.59	-4570.14	90.84	3.21	131.98	2.55	0.09
20	-26039.55	129.30	4.57	-4676.99	101.81	3.60	136.95	2.02	0.07
22	-26018.49	145.87	5.16	-4666.65	109.76	3.88	134.99	2.91	0.10
31	-25970.35	126.65	4.48	-4726.50	94.28	3.33	135.27	2.10	0.07
32	-26012.22	91.49	3.23	-4658.35	82.23	2.91	134.34	2.56	0.09
34	-25979.75	111.29	3.93	-4719.61	91.82	3.25	137.68	2.80	0.10
39	-26167.21	154.91	5.48	-4537.97	131.57	4.65	129.64	3.11	0.11
41	-25909.06	112.08	3.96	-4759.05	89.69	3.17	135.01	2.35	0.08
46	-26068.33	145.74	5.15	-4606.14	94.68	3.35	132.87	1.83	0.06
49	-26359.78	165.35	5.85	-4388.91	138.75	4.91	131.05	4.40	0.16

Pose #	G gas			G solv			TOTAL		
	Avg	Std. Dev.	Std. Err. of Mean	Avg	Std. Dev.	Std. Err. of Mean	Avg	Std. Dev.	Std. Err. of Mean
1	-21063.32	124.37	4.40	-4419.25	91.04	3.22	-25482.58	65.54	2.32
4	-20871.43	175.89	6.22	-4555.97	117.29	4.15	-25427.40	68.55	2.42
7	-21128.10	151.61	5.36	-4349.00	99.20	3.51	-25477.10	59.22	2.09
15	-20856.39	120.43	4.26	-4568.40	96.62	3.42	-25424.78	63.01	2.23
19	-20988.41	144.74	5.12	-4438.16	90.87	3.21	-25426.57	62.44	2.21
20	-20874.75	142.84	5.05	-4540.04	101.83	3.60	-25414.79	59.13	2.09
22	-20864.42	158.83	5.62	-4531.67	109.80	3.88	-25396.09	65.14	2.30
31	-20842.89	141.15	4.99	-4591.23	94.30	3.33	-25434.13	57.72	2.04
32	-20873.01	111.59	3.95	-4524.01	82.27	2.91	-25397.02	59.86	2.12
34	-20821.79	128.95	4.56	-4581.93	91.86	3.25	-25403.72	59.90	2.12
39	-21061.72	166.77	5.90	-4408.34	131.61	4.65	-25470.06	62.97	2.23
41	-20784.32	127.92	4.52	-4624.03	89.73	3.17	-25408.35	56.49	2.00
46	-20924.77	158.57	5.61	-4473.28	94.69	3.35	-25398.05	62.16	2.20
49	-21232.02	177.86	6.29	-4257.86	138.82	4.91	-25489.88	70.22	2.48

STable 10: Total free energy and decomposition of contributions of the receptor, JNK1, used in (+)-zuonin A binding free energy calculations

JNK1 (Receptor)

Pose #	BOND			ANGLE			DIHED			VDWAALS		
	Avg	Std. Dev.	Std. Err. of Mean	Avg	Std. Dev.	Std. Err. of Mean	Avg	Std. Dev.	Std. Err. of Mean	Avg	Std. Dev.	Std. Err. of Mean
1	1102.40	28.42	1.00	3008.38	41.81	1.48	3808.96	26.28	0.93	-2851.44	27.05	0.96
4	1103.84	27.96	0.99	3003.91	43.46	1.54	3808.30	26.10	0.92	-2820.15	28.21	1.00
7	1103.87	27.79	0.98	3017.49	41.97	1.48	3816.03	25.43	0.90	-2842.33	25.19	0.89
15	1104.66	28.65	1.01	3011.30	40.14	1.42	3810.14	25.37	0.90	-2835.97	28.94	1.02
19	1104.59	27.49	0.97	3008.59	43.55	1.54	3806.24	24.63	0.87	-2852.21	28.77	1.02
20	1105.88	28.55	1.01	3009.62	41.10	1.45	3802.83	25.13	0.89	-2810.19	23.29	0.82
22	1105.73	29.63	1.05	3009.86	41.17	1.46	3808.93	24.74	0.87	-2829.26	26.88	0.95
31	1101.62	29.32	1.04	2997.07	42.38	1.50	3816.00	24.57	0.87	-2844.17	24.72	0.87
32	1105.81	27.75	0.98	3010.67	42.50	1.50	3800.88	26.51	0.94	-2825.89	27.41	0.97
34	1107.36	27.88	0.99	3010.74	42.55	1.50	3788.68	26.40	0.93	-2804.03	29.94	1.06
39	1104.64	26.89	0.95	3004.83	41.73	1.48	3811.22	23.42	0.83	-2858.98	27.35	0.97
41	1101.51	27.56	0.97	3001.69	42.38	1.50	3815.22	23.51	0.83	-2842.72	25.69	0.91
46	1104.90	28.66	1.01	3007.64	42.12	1.49	3815.79	27.24	0.96	-2829.86	23.22	0.82
49	1104.00	27.57	0.97	3003.01	40.21	1.42	3814.78	25.14	0.89	-2840.98	35.31	1.25

Pose #	EEL			EGB			ESURF		
	Avg	Std. Dev.	Std. Err. of Mean	Avg	Std. Dev.	Std. Err. of Mean	Avg	Std. Dev.	Std. Err. of Mean
1	-26101.34	106.64	3.77	-4550.31	91.30	3.23	131.56	2.91	0.10
4	-25938.67	163.77	5.79	-4690.66	116.96	4.14	135.96	2.36	0.08
7	-26192.31	138.74	4.91	-4477.40	99.49	3.52	130.34	2.35	0.08
15	-25921.63	103.10	3.65	-4701.37	96.54	3.41	133.73	2.53	0.09
19	-26025.05	129.55	4.58	-4569.99	90.60	3.20	131.89	2.56	0.09
20	-25954.77	129.26	4.57	-4675.35	101.88	3.60	136.88	1.99	0.07
22	-25932.70	146.36	5.17	-4663.00	110.39	3.90	134.53	2.96	0.10
31	-25887.86	126.06	4.46	-4724.16	94.19	3.33	134.99	2.07	0.07
32	-25926.55	91.13	3.22	-4656.39	81.81	2.89	135.24	2.56	0.09
34	-25895.11	111.27	3.93	-4718.77	91.66	3.24	137.71	2.75	0.10
39	-26078.93	155.48	5.50	-4538.28	132.51	4.69	130.95	3.07	0.11
41	-25820.86	111.71	3.95	-4761.30	89.74	3.17	135.88	2.37	0.08
46	-25982.30	146.09	5.17	-4604.19	94.85	3.35	133.99	1.79	0.06
49	-26274.17	165.67	5.86	-4386.84	138.99	4.91	132.03	4.45	0.16

Pose #	G gas			G solv			TOTAL		
	Avg	Std. Dev.	Std. Err. of Mean	Avg	Std. Dev.	Std. Err. of Mean	Avg	Std. Dev.	Std. Err. of Mean
1	-21033.04	123.90	4.38	-4418.75	91.35	3.23	-25451.79	65.45	2.31
4	-20842.78	175.98	6.22	-4554.70	116.98	4.14	-25397.48	67.87	2.40
7	-21097.25	151.87	5.37	-4347.06	99.51	3.52	-25444.30	58.89	2.08
15	-20831.50	120.59	4.26	-4567.64	96.58	3.41	-25399.14	62.98	2.23
19	-20957.84	144.46	5.11	-4438.11	90.64	3.20	-25395.95	62.42	2.21
20	-20846.64	142.78	5.05	-4538.47	101.90	3.60	-25385.11	59.21	2.09
22	-20837.44	159.15	5.63	-4528.47	110.42	3.90	-25365.91	64.56	2.28
31	-20817.34	140.58	4.97	-4589.17	94.21	3.33	-25406.51	57.79	2.04
32	-20835.08	111.06	3.93	-4521.15	81.85	2.89	-25356.23	59.53	2.10
34	-20792.36	128.70	4.55	-4581.06	91.70	3.24	-25373.41	59.35	2.10
39	-21017.21	167.14	5.91	-4407.32	132.55	4.69	-25424.53	62.39	2.21
41	-20745.15	127.47	4.51	-4625.42	89.77	3.17	-25370.58	56.71	2.01
46	-20883.83	158.80	5.61	-4470.20	94.87	3.35	-25354.03	61.65	2.18
49	-21193.36	178.05	6.30	-4254.81	139.06	4.92	-25448.17	70.34	2.49

STable 11: Total free energy and decomposition of contributions of the ligand, (+)-zuonin A, used in (+)-zuonin A binding free energy calculations

(+)-Zuonin A (Ligand)

	BOND			ANGLE			DIHED			VDWAALS		
Pose #	Avg	Std. Dev.	Std. Err. of Mean	Avg	Std. Dev.	Std. Err. of Mean	Avg	Std. Dev.	Std. Err. of Mean	Avg	Std. Dev.	Std. Err. of Mean
1	11.48	2.93	0.10	48.70	3.83	0.14	22.74	2.28	0.08	-3.49	0.98	0.03
4	11.35	2.87	0.10	48.27	4.02	0.14	22.93	2.30	0.08	-3.22	1.03	0.04
7	11.43	2.83	0.10	48.44	3.98	0.14	22.71	2.20	0.08	-3.42	0.94	0.03
15	11.53	2.89	0.10	48.08	4.01	0.14	23.21	2.34	0.08	-3.39	0.96	0.03
19	11.12	2.83	0.10	48.35	3.68	0.13	22.83	2.18	0.08	-3.56	0.95	0.03
20	11.49	2.80	0.10	48.33	3.68	0.13	23.03	2.34	0.08	-3.57	0.97	0.03
22	11.38	2.82	0.10	48.13	3.74	0.13	22.77	2.11	0.07	-3.72	0.92	0.03
31	11.19	2.77	0.10	48.44	3.77	0.13	22.84	2.29	0.08	-3.56	0.98	0.03
32	11.24	2.83	0.10	47.96	3.72	0.13	22.88	2.14	0.08	-3.69	0.92	0.03
34	11.37	2.91	0.10	48.66	3.78	0.13	22.64	2.21	0.08	-3.48	0.95	0.03
39	11.32	2.82	0.10	47.60	3.79	0.13	23.10	2.24	0.08	-3.68	0.88	0.03
41	11.27	2.65	0.09	48.16	3.76	0.13	23.26	2.23	0.08	-3.62	0.92	0.03
46	11.39	2.81	0.10	47.64	3.75	0.13	23.08	2.16	0.08	-3.66	0.93	0.03
49	11.35	2.89	0.10	47.81	3.65	0.13	23.17	2.27	0.08	-3.62	0.91	0.03

	EEL			EGB			ESURF		
Pose #	Avg	Std. Dev.	Std. Err. of Mean	Avg	Std. Dev.	Std. Err. of Mean	Avg	Std. Dev.	Std. Err. of Mean
1	-82.67	2.39	0.08	-13.53	0.50	0.02	2.79	0.02	0.00
4	-83.37	2.84	0.10	-13.43	0.53	0.02	2.78	0.02	0.00
7	-84.75	1.86	0.07	-13.33	0.47	0.02	2.79	0.02	0.00
15	-78.57	1.70	0.06	-13.96	0.48	0.02	2.78	0.02	0.00
19	-82.11	2.25	0.08	-13.71	0.50	0.02	2.79	0.02	0.00
20	-82.35	2.33	0.08	-13.62	0.50	0.02	2.79	0.02	0.00
22	-83.72	1.82	0.06	-13.52	0.48	0.02	2.79	0.02	0.00
31	-79.36	2.00	0.07	-13.75	0.43	0.02	2.78	0.02	0.00
32	-84.36	1.56	0.06	-13.41	0.45	0.02	2.79	0.02	0.00
34	-81.87	2.19	0.08	-13.59	0.48	0.02	2.79	0.02	0.00
39	-84.35	1.48	0.05	-13.37	0.40	0.01	2.79	0.02	0.00
41	-82.71	2.31	0.08	-13.49	0.47	0.02	2.79	0.02	0.00
46	-84.27	1.55	0.05	-13.40	0.43	0.02	2.79	0.02	0.00
49	-84.33	1.58	0.06	-13.40	0.42	0.01	2.78	0.02	0.00

	G gas			G solv			TOTAL		
Pose #	Avg	Std. Dev.	Std. Err. of Mean	Avg	Std. Dev.	Std. Err. of Mean	Avg	Std. Dev.	Std. Err. of Mean
1	-3.23	5.93	0.21	-10.74	0.50	0.02	-13.98	4.57	0.16
4	-4.04	6.23	0.22	-10.65	0.53	0.02	-14.69	4.81	0.17
7	-5.60	5.75	0.20	-10.54	0.47	0.02	-16.14	4.46	0.16
15	0.86	5.80	0.21	-11.18	0.48	0.02	-10.32	4.74	0.17
19	-3.37	5.68	0.20	-10.92	0.50	0.02	-14.28	4.55	0.16
20	-3.07	5.76	0.20	-10.84	0.50	0.02	-13.91	4.72	0.17
22	-5.16	5.53	0.20	-10.74	0.48	0.02	-15.90	4.61	0.16
31	-0.44	5.66	0.20	-10.97	0.44	0.02	-11.41	4.75	0.17
32	-5.97	5.44	0.19	-10.62	0.45	0.02	-16.59	4.44	0.16
34	-2.68	5.78	0.20	-10.80	0.48	0.02	-13.48	4.51	0.16
39	-6.02	5.50	0.19	-10.59	0.40	0.01	-16.61	4.57	0.16
41	-3.64	5.68	0.20	-10.70	0.47	0.02	-14.34	4.65	0.16
46	-5.81	5.47	0.19	-10.62	0.43	0.02	-16.43	4.58	0.16
49	-5.63	5.49	0.19	-10.62	0.42	0.01	-16.24	4.49	0.16

STable 12: Binding free energy of (+)-zuonin A to JNK1 calculated by taking the difference of Complex-Receptor-Ligand

Difference (Complex - Receptor - Ligand) [(+)-Zuonin A/JNK1]

	BOND			ANGLE			DIHED			VDWAALS		
Pose #	Avg	Std. Dev.	Std. Err. of Mean	Avg	Std. Dev.	Std. Err. of Mean	Avg	Std. Dev.	Std. Err. of Mean	Avg	Std. Dev.	Std. Err. of Mean
1	0.00	0.00	0.00	0.00	0.00	0.00	0.00	0.01	0.00	-24.04	2.99	0.11
4	0.00	0.00	0.00	0.00	0.00	0.00	0.00	0.01	0.00	-22.31	2.71	0.10
7	0.00	0.00	0.00	0.00	0.00	0.00	0.00	0.01	0.00	-24.17	2.44	0.09
15	0.00	0.00	0.00	0.00	0.00	0.00	0.00	0.01	0.00	-21.96	2.73	0.10
19	0.00	0.00	0.00	0.00	0.00	0.00	0.00	0.01	0.00	-23.12	2.67	0.09
20	0.00	0.00	0.00	0.00	0.00	0.00	0.00	0.01	0.00	-22.61	3.09	0.11
22	0.00	0.00	0.00	0.00	0.00	0.00	0.00	0.01	0.00	-19.75	1.91	0.07
31	0.00	0.00	0.00	0.00	0.00	0.00	0.00	0.01	0.00	-21.98	2.38	0.08
32	0.00	0.00	0.00	0.00	0.00	0.00	0.00	0.01	0.00	-30.65	3.60	0.13
34	0.00	0.00	0.00	0.00	0.00	0.00	0.00	0.01	0.00	-23.98	2.91	0.10
39	0.00	0.00	0.00	0.00	0.00	0.00	0.00	0.01	0.00	-34.56	3.17	0.11
41	0.00	0.00	0.00	0.00	0.00	0.00	0.00	0.01	0.00	-30.04	2.69	0.10
46	0.00	0.00	0.00	0.00	0.00	0.00	0.00	0.01	0.00	-33.37	3.58	0.13
49	0.00	0.00	0.00	0.00	0.00	0.00	0.00	0.01	0.00	-31.76	2.90	0.10

	EEL			EGB			ESURF		
Pose #	Avg	Std. Dev.	Std. Err. of Mean	Avg	Std. Dev.	Std. Err. of Mean	Avg	Std. Dev.	Std. Err. of Mean
1	-3.01	2.23	0.08	13.08	1.98	0.07	-2.84	0.25	0.01
4	-2.30	2.82	0.10	11.96	2.86	0.10	-2.57	0.29	0.01
7	-1.09	1.94	0.07	11.39	1.70	0.06	-2.79	0.21	0.01
15	-3.79	2.42	0.09	13.06	2.50	0.09	-2.63	0.26	0.01
19	-4.07	2.18	0.08	13.56	2.40	0.08	-2.69	0.24	0.01
20	-2.43	2.19	0.08	11.99	2.11	0.07	-2.72	0.28	0.01
22	-2.08	2.66	0.09	9.87	2.63	0.09	-2.33	0.23	0.01
31	-3.13	2.28	0.08	11.41	2.58	0.09	-2.50	0.28	0.01
32	-1.31	1.84	0.07	11.45	1.87	0.07	-3.69	0.36	0.01
34	-2.77	2.29	0.08	12.75	2.02	0.07	-2.82	0.24	0.01
39	-3.93	3.83	0.14	13.68	3.81	0.13	-4.10	0.30	0.01
41	-5.49	2.25	0.08	15.74	2.25	0.08	-3.65	0.35	0.01
46	-1.76	2.01	0.07	11.45	1.50	0.05	-3.91	0.29	0.01
49	-1.28	2.02	0.07	11.33	1.53	0.05	-3.76	0.24	0.01

	ΔG gas			ΔG solv			ΔG binding		
Pose #	Avg	Std. Dev.	Std. Err. of Mean	Avg	Std. Dev.	Std. Err. of Mean	Avg	Std. Dev.	Std. Err. of Mean
1	-27.05	3.73	0.13	10.24	1.99	0.07	-16.81	2.38	0.08
4	-24.62	3.91	0.14	9.39	2.88	0.10	-15.23	2.28	0.08
7	-25.26	3.12	0.11	8.60	1.71	0.06	-16.66	2.04	0.07
15	-25.75	3.65	0.13	10.42	2.51	0.09	-15.33	2.34	0.08
19	-27.20	3.45	0.12	10.87	2.41	0.09	-16.33	2.27	0.08
20	-25.04	3.79	0.13	9.27	2.13	0.08	-15.77	2.38	0.08
22	-21.82	3.27	0.12	7.54	2.64	0.09	-14.28	1.79	0.06
31	-25.11	3.29	0.12	8.90	2.60	0.09	-16.20	2.02	0.07
32	-31.96	4.04	0.14	7.76	1.91	0.07	-24.20	3.47	0.12
34	-26.75	3.71	0.13	9.93	2.03	0.07	-16.82	2.49	0.09
39	-38.49	4.97	0.18	9.58	3.82	0.14	-28.92	3.09	0.11
41	-35.53	3.51	0.12	12.09	2.27	0.08	-23.43	2.64	0.09
46	-35.13	4.10	0.15	7.54	1.53	0.05	-27.59	3.56	0.13
49	-33.03	3.54	0.13	7.57	1.55	0.05	-25.46	3.00	0.11

STable 13: Total binding free energy contributions calculated from 4-8ns for (-)-zuonin A pose **43** and (+)-zuonin A pose **46**

Complex

Energy Component	(-)-Zuonin A pose **43** Average	Std. Dev.	Std. Err. of Mean	(+)-Zuonin A pose **46** Average	Std. Dev.	Std. Err. of Mean
BOND	1115.96	29.54	1.58	1116.78	28.66	1.53
ANGLE	3051.22	41.79	2.23	3059.31	43.41	2.32
DIHED	3825.08	24.66	1.32	3821.00	23.26	1.24
VDWAALS	-2867.76	23.86	1.28	-2880.53	24.73	1.32
EEL	-26167.71	112.17	6.00	-26158.62	121.20	6.48
1-4 VDW	1339.32	16.51	0.88	1339.80	16.22	0.87
1-4 EEL	15921.76	43.47	2.32	16008.82	51.10	2.73
EGB	-4549.74	85.67	4.58	-4613.13	82.21	4.39
ESURF	136.35	1.60	0.09	134.11	2.16	0.12
G gas	-3782.13	109.81	5.87	-3693.45	102.21	5.46
G solv	-4413.39	84.93	4.54	-4479.02	82.55	4.41
TOTAL	-8195.51	55.02	2.94	-8172.47	53.45	2.86

Receptor (JNK1)

Energy Component	(-)-Zuonin A pose **43** Average	Std. Dev.	Std. Err. of Mean	(+)-Zuonin A pose **46** Average	Std. Dev.	Std. Err. of Mean
BOND	1104.75	29.43	1.57	1105.35	28.60	1.53
ANGLE	3003.89	41.58	2.22	3011.55	43.22	2.31
DIHED	3801.72	24.62	1.32	3798.01	23.18	1.24
VDWAALS	-2828.78	23.84	1.27	-2838.42	24.56	1.31
EEL	-26082.24	112.05	5.99	-26046.53	121.13	6.47
1-4 VDW	1328.44	16.52	0.88	1329.00	16.13	0.86
1-4 EEL	15783.83	43.34	2.32	15831.87	51.11	2.73
EGB	-4547.60	85.72	4.58	-4617.98	82.17	4.39
ESURF	136.99	1.58	0.08	134.96	2.15	0.11
G gas	-3888.39	109.30	5.84	-3809.17	102.05	5.45
G solv	-4410.62	85.02	4.54	-4483.03	82.49	4.41
TOTAL	-8299.01	54.72	2.92	-8292.19	53.09	2.84

Ligand (Zuonin A)

Energy Component	(-)-Zuonin A pose **43** Average	Std. Dev.	Std. Err. of Mean	(+)-Zuonin A pose **46** Average	Std. Dev.	Std. Err. of Mean
BOND	11.21	2.76	0.15	11.42	2.90	0.16
ANGLE	47.33	3.70	0.20	47.75	3.84	0.21
DIHED	23.36	2.13	0.11	22.99	2.00	0.11
VDWAALS	-3.67	0.89	0.05	-3.82	0.80	0.04
EEL	-84.08	1.45	0.08	-103.65	1.55	0.08
1-4 VDW	10.88	1.00	0.05	10.79	0.99	0.05
1-4 EEL	137.93	1.63	0.09	176.95	1.74	0.09
EGB	-13.44	0.41	0.02	-14.78	0.44	0.02
ESURF	4.16	0.03	0.00	4.16	0.03	0.00
G gas	142.96	4.55	0.24	162.43	4.70	0.25
G solv	-9.28	0.40	0.02	-10.62	0.43	0.02
TOTAL	133.68	4.56	0.24	151.81	4.67	0.25

Difference (Complex - Receptor - Ligand)

Energy Component	(-)-Zuonin A pose **43** Average	Std. Dev.	Std. Err. of Mean	(+)-Zuonin A pose **46** Average	Std. Dev.	Std. Err. of Mean
BOND	0.00	0.00	0.00	0.00	0.00	0.00
ANGLE	0.00	0.00	0.00	0.00	0.00	0.00
DIHED	0.00	0.01	0.00	0.00	0.01	0.00
VDWAALS	-35.31	2.35	0.13	-38.29	2.31	0.12
EEL	-1.39	2.02	0.11	-8.43	2.03	0.11
1-4 VDW	0.00	0.00	0.00	0.00	0.00	0.00
1-4 EEL	0.00	0.00	0.00	0.00	0.00	0.00
EGB	11.30	1.49	0.08	19.63	1.72	0.09
ESURF	-4.79	0.19	0.01	-5.00	0.13	0.01
DELTA G gas	-36.70	3.11	0.17	-46.72	3.22	0.17
DELTA G solv	6.51	1.42	0.08	14.63	1.67	0.09
DELTA TOTAL	-30.19	2.43	0.13	-32.09	2.38	0.13

STable 14: Decomposition of (-)-zuonin A binding free energy contributions from individual JNK1 residues (side chain + backbone) taken from 4-8ns

(-)-Zuonin A/JNK Binding Free Energy Decomposition (Backbone + Side Chain)																
Residue	Internal			van der Waals			Electrostatic			Polar Solvation			Non-Polar Solv.			TOTAL		
	Avg.	Std. Dev.	Std. Err. of Mean	Avg.	Std. Dev.	Std. Err. of Mean	Avg.	Std. Dev.	Std. Err. of Mean	Avg.	Std. Dev.	Std. Err. of Mean	Avg.	Std. Dev.	Std. Err. of Mean	Avg.	Std. Dev.	Std. Err. of Mean
ASP112	0.000	0.000	0.000	-0.435	0.156	0.008	-0.587	0.221	0.012	0.991	0.285	0.015	-0.052	0.020	0.001	-0.082	0.103	0.006
ALA113	0.000	0.000	0.000	-0.384	0.136	0.007	-0.056	0.026	0.001	0.111	0.032	0.002	-0.053	0.021	0.001	-0.382	0.143	0.008
ASN114	0.000	0.000	0.000	-0.089	0.020	0.001	0.056	0.039	0.002	-0.009	0.039	0.002	0.000	0.000	0.000	-0.042	0.018	0.001
LEU115	0.000	0.000	0.000	-0.645	0.201	0.011	0.062	0.080	0.004	-0.044	0.055	0.003	-0.024	0.010	0.001	-0.652	0.197	0.011
CYS116	0.000	0.000	0.000	-0.038	0.006	0.000	0.002	0.011	0.001	0.027	0.013	0.001	0.000	0.000	0.000	-0.009	0.006	0.000
GLN117	0.000	0.000	0.000	-0.087	0.021	0.001	-0.035	0.029	0.002	0.120	0.044	0.002	0.000	0.000	0.000	-0.003	0.014	0.001
VAL118	0.000	0.000	0.000	-1.719	0.434	0.023	-0.395	0.253	0.014	0.563	0.152	0.008	-0.237	0.043	0.002	-1.787	0.460	0.025
ILE119	0.000	0.000	0.000	-0.864	0.205	0.011	-0.380	0.237	0.013	0.427	0.180	0.010	-0.027	0.011	0.001	-0.845	0.251	0.013
GLN120	0.000	0.000	0.000	-0.168	0.066	0.004	0.047	0.057	0.003	0.018	0.036	0.002	0.000	0.000	0.000	-0.102	0.047	0.003
MET121	0.000	0.000	0.000	-0.897	0.360	0.019	-0.690	0.376	0.020	0.758	0.323	0.017	-0.071	0.053	0.003	-0.900	0.405	0.022
GLU122	0.000	0.000	0.000	-0.339	0.151	0.008	0.798	0.325	0.017	-0.339	0.265	0.014	-0.021	0.016	0.001	0.099	0.099	0.005
LEU123	0.000	0.000	0.000	-1.364	0.345	0.018	-0.211	0.090	0.005	0.296	0.074	0.004	-0.173	0.030	0.002	-1.452	0.358	0.019
ASP124	0.000	0.000	0.000	-0.074	0.021	0.001	0.939	0.294	0.016	-0.820	0.267	0.014	0.000	0.000	0.000	0.045	0.035	0.002
HIE125	0.000	0.000	0.000	-0.017	0.003	0.000	0.047	0.023	0.001	-0.034	0.022	0.001	0.000	0.000	0.000	-0.005	0.003	0.000
GLU126	0.000	0.000	0.000	-0.028	0.006	0.000	0.386	0.130	0.007	-0.329	0.126	0.007	0.000	0.000	0.000	0.029	0.012	0.001
ARG127	0.000	0.000	0.000	-2.168	0.422	0.023	-3.704	0.821	0.044	4.632	0.817	0.044	-0.384	0.053	0.003	-1.623	0.501	0.027
MET128	0.000	0.000	0.000	-0.102	0.021	0.001	-0.005	0.033	0.002	0.035	0.031	0.002	0.000	0.000	0.000	-0.071	0.017	0.001
SER129	0.000	0.000	0.000	-0.015	0.002	0.000	-0.022	0.020	0.001	0.027	0.021	0.001	0.000	0.000	0.000	-0.010	0.003	0.000
TYR130	0.000	0.000	0.000	-0.073	0.015	0.001	-0.124	0.028	0.001	0.147	0.029	0.002	0.000	0.000	0.000	-0.050	0.013	0.001
LEU131	0.000	0.000	0.000	-0.970	0.304	0.016	-0.106	0.055	0.003	0.152	0.050	0.003	-0.083	0.021	0.001	-1.008	0.315	0.017
LEU132	0.000	0.000	0.000	-0.026	0.006	0.000	-0.040	0.012	0.001	0.046	0.012	0.001	0.000	0.000	0.000	-0.021	0.006	0.000
TYR133	0.000	0.000	0.000	-0.009	0.001	0.000	-0.025	0.012	0.001	0.030	0.012	0.001	0.000	0.000	0.000	-0.004	0.002	0.000
GLN134	0.000	0.000	0.000	-0.034	0.005	0.000	-0.103	0.037	0.002	0.105	0.036	0.002	0.000	0.000	0.000	-0.032	0.008	0.000
MET135	0.000	0.000	0.000	-0.033	0.011	0.001	-0.022	0.020	0.001	0.029	0.020	0.001	0.000	0.000	0.000	-0.026	0.010	0.001
VAL159	0.000	0.000	0.000	-1.405	0.269	0.014	0.182	0.055	0.003	0.079	0.068	0.004	-0.114	0.018	0.001	-1.258	0.261	0.014
LYS160	0.000	0.000	0.000	-1.055	0.209	0.011	0.072	0.249	0.013	0.143	0.231	0.012	-0.056	0.013	0.001	-0.897	0.208	0.011
SER161	0.000	0.000	0.000	-2.130	0.416	0.022	-0.346	0.382	0.020	1.476	0.360	0.019	-0.361	0.030	0.002	-1.361	0.526	0.028
ASP162	0.000	0.000	0.000	-1.120	0.252	0.013	-0.183	0.233	0.012	0.364	0.278	0.015	-0.086	0.025	0.001	-1.026	0.293	0.016
CYS163	0.000	0.000	0.000	-1.514	0.338	0.018	0.267	0.320	0.017	0.135	0.221	0.012	-0.131	0.023	0.001	-1.243	0.295	0.016
THR164	0.000	0.000	0.000	-0.181	0.035	0.002	-0.229	0.057	0.003	0.222	0.047	0.003	0.000	0.000	0.000	-0.187	0.051	0.003
LEU165	0.000	0.000	0.000	-0.131	0.036	0.002	0.035	0.018	0.001	-0.021	0.016	0.001	0.000	0.000	0.000	-0.117	0.034	0.002
MET218	0.000	0.000	0.000	-0.473	0.180	0.010	-0.125	0.102	0.005	0.158	0.061	0.003	-0.011	0.009	0.000	-0.451	0.195	0.010
ZA-	0.001	0.008	0.000	-19.144	1.154	0.062	-4.214	1.015	0.054	9.774	0.805	0.043	-3.117	0.087	0.005	-16.700	1.233	0.066

STable 15: Decomposition of (-)-zuonin A binding free energy contributions from individual JNK1 residues (side chain only) taken from 4-8ns

(-)-Zuonin A/JNK Binding Free Energy Decomposition (Side chain)																		
Residue	Internal			van der Waals			Electrostatic			Polar Solvation			Non-Polar Solv.			TOTAL		
	Avg.	Std. Dev.	Std. Err. of Mean	Avg.	Std. Dev.	Std. Err. of Mean	Avg.	Std. Dev.	Std. Err. of Mean	Avg.	Std. Dev.	Std. Err. of Mean	Avg.	Std. Dev.	Std. Err. of Mean	Avg.	Std. Dev.	Std. Err. of Mean
ASP112	0.000	0.000	0.000	-0.311	0.119	0.006	-0.558	0.219	0.012	0.891	0.280	0.015	-0.051	0.020	0.001	-0.029	0.088	0.005
ALA113	0.000	0.000	0.000	-0.219	0.119	0.006	0.001	0.006	0.000	0.003	0.006	0.000	-0.053	0.021	0.001	-0.269	0.128	0.007
ASN114	0.000	0.000	0.000	-0.015	0.003	0.000	0.028	0.017	0.001	-0.013	0.017	0.001	0.000	0.000	0.000	0.000	0.004	0.000
LEU115	0.000	0.000	0.000	-0.494	0.197	0.011	-0.032	0.051	0.003	0.033	0.026	0.001	-0.024	0.010	0.001	-0.516	0.184	0.010
CYS116	0.000	0.000	0.000	-0.007	0.001	0.000	-0.001	0.006	0.000	0.004	0.006	0.000	0.000	0.000	0.000	-0.005	0.002	0.000
GLN117	0.000	0.000	0.000	-0.032	0.015	0.001	-0.014	0.023	0.001	0.056	0.037	0.002	0.000	0.000	0.000	0.010	0.008	0.000
VAL118	0.000	0.000	0.000	-1.269	0.304	0.016	-0.106	0.086	0.005	0.084	0.065	0.003	-0.211	0.045	0.002	-1.502	0.325	0.017
ILE119	0.000	0.000	0.000	-0.254	0.078	0.004	-0.048	0.046	0.002	0.038	0.026	0.001	0.000	0.002	0.000	-0.265	0.089	0.005
GLN120	0.000	0.000	0.000	-0.024	0.007	0.000	0.006	0.015	0.001	0.018	0.015	0.001	0.000	0.000	0.000	0.001	0.004	0.000
MET121	0.000	0.000	0.000	-0.428	0.229	0.012	-0.015	0.095	0.005	0.065	0.074	0.004	-0.061	0.053	0.003	-0.439	0.260	0.014
GLU122	0.000	0.000	0.000	-0.033	0.012	0.001	0.268	0.134	0.007	-0.195	0.127	0.007	0.000	0.000	0.000	0.040	0.010	0.001
LEU123	0.000	0.000	0.000	-1.210	0.330	0.018	-0.076	0.068	0.004	0.126	0.044	0.002	-0.172	0.030	0.002	-1.332	0.345	0.018
ASP124	0.000	0.000	0.000	-0.029	0.011	0.001	0.746	0.255	0.014	-0.650	0.230	0.012	0.000	0.000	0.000	0.068	0.030	0.002
HIE125	0.000	0.000	0.000	-0.006	0.001	0.000	0.015	0.012	0.001	-0.006	0.011	0.001	0.000	0.000	0.000	0.003	0.001	0.000
GLU126	0.000	0.000	0.000	-0.009	0.002	0.000	0.334	0.109	0.006	-0.298	0.105	0.006	0.000	0.000	0.000	0.027	0.011	0.001
ARG127	0.000	0.000	0.000	-2.083	0.413	0.022	-3.709	0.818	0.044	4.593	0.815	0.044	-0.384	0.053	0.003	-1.583	0.493	0.026
MET128	0.000	0.000	0.000	-0.050	0.013	0.001	-0.043	0.027	0.001	0.053	0.025	0.001	0.000	0.000	0.000	-0.040	0.012	0.001
SER129	0.000	0.000	0.000	-0.003	0.001	0.000	-0.010	0.019	0.001	0.016	0.019	0.001	0.000	0.000	0.000	0.002	0.002	0.000
TYR130	0.000	0.000	0.000	-0.053	0.013	0.001	-0.044	0.012	0.001	0.079	0.016	0.001	0.000	0.000	0.000	-0.018	0.008	0.000
LEU131	0.000	0.000	0.000	-0.921	0.301	0.016	-0.053	0.050	0.003	0.098	0.043	0.002	-0.083	0.021	0.001	-0.959	0.312	0.017
LEU132	0.000	0.000	0.000	-0.013	0.005	0.000	-0.023	0.009	0.000	0.023	0.009	0.000	0.000	0.000	0.000	-0.014	0.005	0.000
TYR133	0.000	0.000	0.000	-0.005	0.001	0.000	-0.006	0.006	0.000	0.011	0.006	0.000	0.000	0.000	0.000	0.000	0.001	0.000
GLN134	0.000	0.000	0.000	-0.029	0.005	0.000	-0.089	0.030	0.002	0.090	0.029	0.002	0.000	0.000	0.000	-0.027	0.007	0.000
MET135	0.000	0.000	0.000	-0.028	0.011	0.001	-0.008	0.017	0.001	0.014	0.017	0.001	0.000	0.000	0.000	-0.022	0.010	0.001
VAL159	0.000	0.000	0.000	-1.047	0.240	0.013	0.152	0.051	0.003	-0.066	0.033	0.002	-0.112	0.018	0.001	-1.073	0.249	0.013
LYS160	0.000	0.000	0.000	-0.109	0.023	0.001	0.327	0.180	0.010	-0.236	0.176	0.009	0.000	0.000	0.000	-0.018	0.023	0.001
SER161	0.000	0.000	0.000	-0.556	0.194	0.010	-0.144	0.108	0.006	0.659	0.221	0.012	-0.107	0.037	0.002	-0.148	0.256	0.014
ASP162	0.000	0.000	0.000	-0.160	0.041	0.002	-0.187	0.228	0.012	0.267	0.225	0.012	-0.001	0.004	0.000	-0.081	0.050	0.003
CYS163	0.000	0.000	0.000	-0.623	0.277	0.015	-0.075	0.220	0.012	0.046	0.183	0.010	-0.085	0.029	0.002	-0.737	0.249	0.013
THR164	0.000	0.000	0.000	-0.036	0.006	0.000	-0.026	0.028	0.001	0.033	0.028	0.001	0.000	0.000	0.000	-0.029	0.010	0.001
LEU165	0.000	0.000	0.000	-0.095	0.030	0.002	0.033	0.015	0.001	-0.026	0.013	0.001	0.000	0.000	0.000	-0.087	0.027	0.001
MET218	0.000	0.000	0.000	-0.419	0.167	0.009	-0.052	0.102	0.005	0.055	0.049	0.003	-0.011	0.009	0.000	-0.427	0.188	0.010
ZA-	0.001	0.008	0.000	-19.144	1.154	0.062	-4.214	1.015	0.054	9.774	0.805	0.043	-3.117	0.087	0.005	-16.700	1.233	0.066

STable 16: Decomposition of (-)-zuonin A binding free energy contributions from individual JNK1 residues (backbone only) taken from 4-8ns

(-)-Zuonin A/JNK Binding Free Energy Decomposition (Backbone)																
Residue	Internal			van der Waals			Electrostatic			Polar Solvation			Non-Polar Solv.			TOTAL		
	Avg.	Std. Dev.	Std. Err. of Mean	Avg.	Std. Dev.	Std. Err. of Mean	Avg.	Std. Dev.	Std. Err. of Mean	Avg.	Std. Dev.	Std. Err. of Mean	Avg.	Std. Dev.	Std. Err. of Mean	Avg.	Std. Dev.	Std. Err. of Mean
ASP112	0.000	0.000	0.000	-0.124	0.047	0.003	-0.029	0.027	0.001	0.100	0.045	0.002	0.000	0.001	0.000	-0.053	0.031	0.002
ALA113	0.000	0.000	0.000	-0.164	0.054	0.003	-0.057	0.024	0.001	0.108	0.030	0.002	0.000	0.000	0.000	-0.113	0.045	0.002
ASN114	0.000	0.000	0.000	-0.074	0.018	0.001	0.028	0.026	0.001	0.004	0.026	0.001	0.000	0.000	0.000	-0.042	0.016	0.001
LEU115	0.000	0.000	0.000	-0.151	0.033	0.002	0.094	0.073	0.004	-0.078	0.058	0.003	0.000	0.000	0.000	-0.135	0.043	0.002
CYS116	0.000	0.000	0.000	-0.031	0.005	0.000	0.003	0.009	0.000	0.024	0.011	0.001	0.000	0.000	0.000	-0.004	0.005	0.000
GLN117	0.000	0.000	0.000	-0.055	0.009	0.000	-0.021	0.016	0.001	0.064	0.019	0.001	0.000	0.000	0.000	-0.013	0.011	0.001
VAL118	0.000	0.000	0.000	-0.450	0.345	0.018	-0.289	0.275	0.015	0.479	0.163	0.009	-0.026	0.013	0.001	-0.286	0.364	0.019
ILE119	0.000	0.000	0.000	-0.610	0.198	0.011	-0.332	0.222	0.012	0.388	0.179	0.010	-0.027	0.010	0.001	-0.580	0.218	0.012
GLN120	0.000	0.000	0.000	-0.144	0.060	0.003	0.041	0.057	0.003	0.000	0.028	0.002	0.000	0.000	0.000	-0.103	0.048	0.003
MET121	0.000	0.000	0.000	-0.469	0.190	0.010	-0.675	0.349	0.019	0.693	0.297	0.016	-0.010	0.007	0.000	-0.461	0.214	0.011
GLU122	0.000	0.000	0.000	-0.306	0.140	0.007	0.530	0.235	0.013	-0.144	0.176	0.009	-0.021	0.016	0.001	0.059	0.097	0.005
LEU123	0.000	0.000	0.000	-0.155	0.056	0.003	-0.135	0.070	0.004	0.171	0.052	0.003	0.000	0.001	0.000	-0.119	0.069	0.004
ASP124	0.000	0.000	0.000	-0.045	0.011	0.001	0.193	0.067	0.004	-0.170	0.062	0.003	0.000	0.000	0.000	-0.023	0.013	0.001
HIE125	0.000	0.000	0.000	-0.012	0.002	0.000	0.032	0.016	0.001	-0.028	0.016	0.001	0.000	0.000	0.000	-0.008	0.003	0.000
GLU126	0.000	0.000	0.000	-0.018	0.004	0.000	0.052	0.030	0.002	-0.031	0.029	0.002	0.000	0.000	0.000	0.002	0.005	0.000
ARG127	0.000	0.000	0.000	-0.084	0.016	0.001	0.005	0.044	0.002	0.039	0.038	0.002	0.000	0.000	0.000	-0.041	0.016	0.001
MET128	0.000	0.000	0.000	-0.052	0.010	0.001	0.038	0.025	0.001	-0.018	0.023	0.001	0.000	0.000	0.000	-0.032	0.007	0.000
SER129	0.000	0.000	0.000	-0.011	0.002	0.000	-0.012	0.009	0.000	0.012	0.009	0.000	0.000	0.000	0.000	-0.012	0.003	0.000
TYR130	0.000	0.000	0.000	-0.020	0.003	0.000	-0.080	0.018	0.001	0.068	0.017	0.001	0.000	0.000	0.000	-0.032	0.006	0.000
LEU131	0.000	0.000	0.000	-0.050	0.009	0.000	-0.053	0.014	0.001	0.054	0.014	0.001	0.000	0.000	0.000	-0.049	0.010	0.001
LEU132	0.000	0.000	0.000	-0.013	0.002	0.000	-0.017	0.008	0.000	0.023	0.007	0.000	0.000	0.000	0.000	-0.007	0.003	0.000
TYR133	0.000	0.000	0.000	-0.004	0.001	0.000	-0.019	0.007	0.000	0.020	0.007	0.000	0.000	0.000	0.000	-0.004	0.001	0.000
GLN134	0.000	0.000	0.000	-0.006	0.001	0.000	-0.014	0.008	0.000	0.014	0.008	0.000	0.000	0.000	0.000	-0.005	0.002	0.000
MET135	0.000	0.000	0.000	-0.004	0.001	0.000	-0.013	0.005	0.000	0.015	0.005	0.000	0.000	0.000	0.000	-0.003	0.001	0.000
VAL159	0.000	0.000	0.000	-0.358	0.103	0.006	0.030	0.062	0.003	0.145	0.071	0.004	-0.002	0.003	0.000	-0.186	0.066	0.004
LYS160	0.000	0.000	0.000	-0.946	0.196	0.010	-0.255	0.192	0.010	0.379	0.178	0.010	-0.056	0.013	0.001	-0.879	0.205	0.011
SER161	0.000	0.000	0.000	-1.573	0.361	0.019	-0.202	0.369	0.020	0.817	0.261	0.014	-0.254	0.025	0.001	-1.213	0.472	0.025
ASP162	0.000	0.000	0.000	-0.960	0.219	0.012	0.004	0.107	0.006	0.097	0.090	0.005	-0.085	0.024	0.001	-0.945	0.266	0.014
CYS163	0.000	0.000	0.000	-0.891	0.165	0.009	0.342	0.227	0.012	0.089	0.152	0.008	-0.046	0.020	0.001	-0.505	0.172	0.009
THR164	0.000	0.000	0.000	-0.145	0.030	0.002	-0.203	0.058	0.003	0.189	0.049	0.003	0.000	0.000	0.000	-0.158	0.045	0.002
LEU165	0.000	0.000	0.000	-0.036	0.007	0.000	0.002	0.020	0.001	0.005	0.019	0.001	0.000	0.000	0.000	-0.030	0.009	0.000
MET218	0.000	0.000	0.000	-0.054	0.023	0.001	-0.073	0.043	0.002	0.102	0.044	0.002	0.000	0.000	0.000	-0.024	0.020	0.001
ZA-	0.000	0.000	0.000	0.000	0.000	0.000	0.000	0.000	0.000	0.000	0.000	0.000	0.000	0.000	0.000	0.000	0.000	0.000

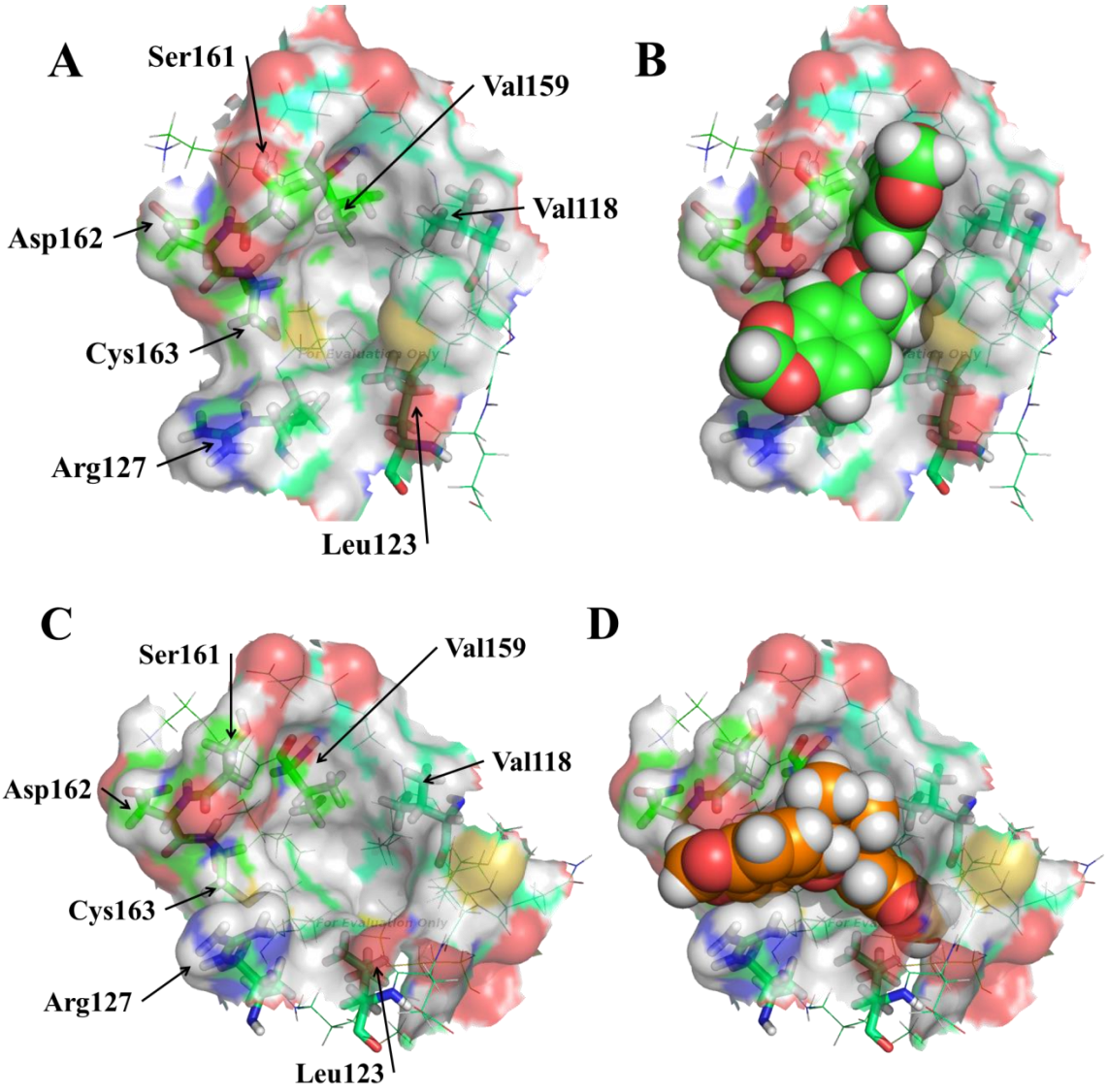

SFigure 11: Stable binding pose of a) (-)-Zuonin A pose **43** and b) (+)-Zuonin A pose **39**. Enlarged version of Figure 10

References

1. Avruch, J., *MAP kinase pathways: The first twenty years.* Biochimica Et Biophysica Acta-Molecular Cell Research, 2007. 1773(8): p. 1150-1160.
2. Bubus12. *Simple overview of mammalian MAPK cascades*. 2012 [cited 2013; Available from: http://commons.wikimedia.org/wiki/File:MAPK-pathway-mammalian.png.
3. Johnson, G.L. and K. Nakamura, *The c-jun kinase/stress-activated pathway: Regulation, function and role in human disease.* Biochimica Et Biophysica Acta-Molecular Cell Research, 2007. 1773(8): p. 1341-1348.
4. Davies, C. and C. Tournier, *Exploring the function of the JNK (c-Jun N-terminal kinase) signalling pathway in physiological and pathological processes to design novel therapeutic strategies.* Biochemical Society Transactions, 2012. 40: p. 85-89.
5. Sabapathy, K., *Role of the JNK Pathway in Human Diseases.* Protein Phosphorylation in Health and Disease, 2012. 106: p. 145-169.
6. Yan, C.L., et al., *Understanding the Specificity of a Docking Interaction between JNK1 and the Scaffolding Protein JIP1.* Journal of Physical Chemistry B, 2011. 115(6): p. 1491-1502.
7. Grewal, S., D.M. Molina, and L. Bardwell, *Mitogen-activated protein kinase (MAPK)-docking sites in MAPK kinases function as tethers that are crucial for MAPK regulation in vivo.* Cellular Signalling, 2006. 18(1): p. 123-134.
8. Heo, J.S., et al., *Structural basis for the selective inhibition of JNK1 by the scaffolding protein JIP1 and SP600125.* Embo Journal, 2004. 23(11): p. 2185-2195.
9. Kirkland, L.O. and C. McInnes, *Non-ATP competitive protein kinase inhibitors as anti-tumor therapeutics.* Biochemical Pharmacology, 2009. 77(10): p. 1561-1571.
10. Kaoud, T.S., et al., *From in Silico Discovery to Intracellular Activity: Targeting JNK-Protein Interactions with Small Molecules.* Acs Medicinal Chemistry Letters, 2012. 3(9): p. 721-725.
11. Kaoud, T.S., et al., *Manipulating JNK Signaling with (-)-Zuonin A.* Acs Chemical Biology, 2012. 7(11): p. 1873-1883.
12. Paul, S.M., et al., *How to improve R&D productivity: the pharmaceutical industry's grand challenge.* Nature Reviews Drug Discovery, 2010. 9(3): p. 203-214.
13. Hartshorn, M.J., et al., *Diverse, high-quality test set for the validation of protein-ligand docking performance.* Journal of Medicinal Chemistry, 2007. 50(4): p. 726-741.

14. M. J. Frisch, G.W.T., H. B. Schlegel, G. E. Scuseria, M. A. Robb, J. R. Cheeseman, G. Scalmani, V. Barone, B. Mennucci, G. A. Petersson, H. Nakatsuji, M. Caricato, X. Li, H. P. Hratchian, A. F. Izmaylov, J. Bloino, G. Zheng, J. L. Sonnenberg, M. Hada, M. Ehara, K. Toyota, R. Fukuda, J. Hasegawa, M. Ishida, T. Nakajima, Y. Honda, O. Kitao, H. Nakai, T. Vreven, J. A. Montgomery, Jr., J. E. Peralta, F. Ogliaro, M. Bearpark, J. J. Heyd, E. Brothers, K. N. Kudin, V. N. Staroverov, R. Kobayashi, J. Normand, K. Raghavachari, A. Rendell, J. C. Burant, S. S. Iyengar, J. Tomasi, M. Cossi, N. Rega, J. M. Millam, M. Klene, J. E. Knox, J. B. Cross, V. Bakken, C. Adamo, J. Jaramillo, R. Gomperts, R. E. Stratmann, O. Yazyev, A. J. Austin, R. Cammi, C. Pomelli, J. W. Ochterski, R. L. Martin, K. Morokuma, V. G. Zakrzewski, G. A. Voth, P. Salvador, J. J. Dannenberg, S. Dapprich, A. D. Daniels, O. Farkas, J. B. Foresman, J. V. Ortiz, J. Cioslowski, and D. J. Fox, *Gaussian 09*, 2009, Gaussian, Inc.: Wallingford, CT.

15. Singh, U.C. and P.A. Kollman, *An Approach to Computing Electrostatic Charges for Molecules.* Journal of Computational Chemistry, 1984. 5(2): p. 129-145.

16. Besler, B.H., K.M. Merz, and P.A. Kollman, *Atomic Charges Derived from Semiempirical Methods.* Journal of Computational Chemistry, 1990. 11(4): p. 431-439.

17. D.A. Case, T.A.D., T.E. Cheatham, III, C.L. Simmerling, J. Wang, R.E. Duke, R. Luo, R.C. Walker, W. Zhang, K.M. Merz, B. Roberts, S. Hayik, A. Roitberg, G. Seabra, J. Swails, A.W. Goetz, I. Kolossváry, K.F. Wong, F. Paesani, J. Vanicek, R.M. Wolf, J. Liu, X. Wu, S.R. Brozell, T. Steinbrecher, H. Gohlke, Q. Cai, X. Ye, J. Wang, M.-J. Hsieh, G. Cui, D.R. Roe, D.H. Mathews, M.G. Seetin, R. Salomon-Ferrer, C. Sagui, V. Babin, T. Luchko, S. Gusarov, A. Kovalenko, and P.A. Kollman, *AMBER 12*, 2012, University of California, San Francisco.

18. Essmann, U., et al., *A Smooth Particle Mesh Ewald Method.* Journal of Chemical Physics, 1995. 103(19): p. 8577-8593.